Fisheries and Oceans Canada | Pêches et Océans Canada
Ecosystems and Oceans Science | Sciences des écosystèmes et des océans

Canadian Science Advisory Secretariat (CSAS)

Research Document 2025/083

Maritimes Region

Stock Assessment Framework for Scallop Fishing Areas 25, 26, and 27B: Reference Points

Keith, D., Keyser, F., McDonald R, Pearo Drew, T., and Sameoto, J.A.

Bedford Institute of Oceanography
Fisheries and Oceans Canada
1 Challenger Drive
Dartmouth, Nova Scotia, Canada, B2Y 4A2

December 2025

Canada

Foreword

This series documents the scientific basis for the evaluation of aquatic resources and ecosystems in Canada. As such, it addresses the issues of the day in the time frames required and the documents it contains are not intended as definitive statements on the subjects addressed but rather as progress reports on ongoing investigations.

Published by:

Fisheries and Oceans Canada
Canadian Science Advisory Secretariat
200 Kent Street
Ottawa ON K1A 0E6

http://www.dfo-mpo.gc.ca/csas-sccs/
DFO.CSAS-SCAS.MPO@dfo-mpo.gc.ca

ISSN 1919-5044
ISBN 978-0-660-95263-5 Cat. No. Fs70-5/2025-083E-PDF

Correct citation for this publication:

Keith, D., Keyser, F., McDonald, R., Pearo Drew, T., and Sameoto, J.A. 2025. Stock Assessment Framework for Scallop Fishing Areas 25, 26, and 27B: Reference Points. DFO Can. Sci. Advis. Sec. Res. Doc. 2025/083. iv + 60 p.

Aussi disponible en français :

Keith, D., Keyser, F., McDonald, R., Pearo Drew, T., Sameoto, J.A. 2025. Cadre d'évaluation des stocks pour les zones de pêche du pétoncle 25, 26 et 27B : points de référence. Secr. can. des avis sci. du MPO. Doc. de rech. 2025/083. iv + 62 p.

TABLE OF CONTENTS

ABSTRACT

This research document focuses on the development of reference points for Scallop Fishing Area (SFA) 25A (Sable Bank), SFA 26A (Browns Bank North), SFA 26C (German Bank), and SFA 27B (Georges Bank 'b'). The survey biomass indices and relative exploitation rates used for the development of the index based reference points were approved during the first of two Canadian Science Advisory Secretariat Regional Peer Review meetings which focused on the data inputs (each of these SFAs) and model development (SFA 25A and SFA 26A). The stock assessment models and the productivity scenarios used for the maximum sustainable yield (MSY) simulations in SFA 25A and SFA 26A were also approved during this initial meeting. Survey biomass index based limit reference points (LRPs) are proposed for each of these SFA's. In addition to the survey index based LRPs, guidance on relative target (RR_{tar}) and limit (RR_{lim}) removal reference and upper stock reference points (USR) is provided for all the areas based on the survey biomass index and relative exploitation rates. In the two areas with approved stock assessment models (SFA 25A and SFA 26A), MSY simulations are used to obtain model based LRPs. Guidance on target removal reference (RR_{tar}) and upper stock reference (USR) points are also provided using the MSY simulations for these two areas. In addition, for the two modelled areas, harvest decision rule (HDR) simulations are developed and their potential use demonstrated using the following example: 1) maintain the stock near the TRP, 2) increase the long term average removals from the fishery above the removals estimated using the optimal MSY simulation, and 3) reduce the proportion of time the stock is below the LRP when compared to the optimal MSY simulation. The HDR simulations are able to identify a scenario in which all three of these management objectives were met, with notable increases in the long-term median removals for both areas and declines in the proportion of the time the stocks are below the LRP. The HDR simulations represent a methodology by which the impact of various management objectives could be explored; this could include the development of limit removal reference (RR_{lim}) and target reference points (TRP). In areas in which model based reference points are available (SFAs 25A and 26A), these are preferred, and an LRP of 40% of the fully-recruited biomass at MSY is recommended. In areas with only index based reference points (SFAs 26C and 27B), an LRP of 30% of the fully-recruited biomass index is recommended.

1. INTRODUCTION

This is the third and final research document stemming from an assessment framework review process focused on scallop fishing areas (SFAs) 25, 26, and 27B. The first research document focused on data inputs (Keyser et al. In press) while the second document developed new assessment models for SFAs 25A and 26A (Keith et al. In press). The SFA 26 management unit also includes 26B (Browns Bank South) and 26C (German Bank), whereas SFA 27 includes both 27A (Georges Bank 'a') and 27B (Georges Bank 'b'), and SFA 25, known as the Eastern Scotian Shelf is split into SFA 25A, which includes 25A-Sab (Sable Bank), 25A-Mid (Middle Bank), and 25B (Banquereau, see Table 1 in Keyser et al. In press).

A history of the survey and fisheries in SFAs 25, 26, and 27B can be found in Keyser et al. (In press). Scallop growth and the selectivity of the fishery varies by area, as such the size categories of scallop varies by area. In both SFA 25A and SFA 26A scallop defined as fully-recruited (FR) are greater than 90 mm in size, recruit scallop are defined as being 75–89 mm in size. In SFA 26C recruit scallop are defined as being between 95–104 mm, while fully-recruited scallop are greater than105 mm. Finally, in SFA 27B, recruit scallop are defined as scallop that are 85–94 mm in size, while fully-recruited scallop are greater than 95 mm (Keyser et al. In press).

The primary fishing area within SFA 26 is SFA 26A (Browns Bank North). In SFA 25, SFA 25A-Sab (Sable Bank) has been the most consistently fished area. The Middle Bank component of this area is excluded from these analyses due to the limited fishing activity in this portion of SFA 25; hereafter, SFA 25A-Sab will be referred to as SFA 25A (Keyser et al. In press). A Bayesian State-Space delay difference model (BSSM) has been adopted for SFA 25A, while a new Spatially Explicit Stock Assessment Model (SEAM) has been adopted for SFA 26A (Keith et al. In press). In addition, to minimize prediction bias, the productivity parameters used to project biomass into future years differed between these two areas; however, in both areas the projections used the same non-spatial version of the delay difference model (Keith et al. In press). In SFA 25A, for one-year ahead projections the previous year's natural mortality, recruitment, and recruit growth are used and the fully-recruited growth term is set to one (i.e., the projections assume no full-recruited growth). In SFA 26A, for one-year ahead projections, the previous year's natural mortality, recruitment, recruit growth, and fully-recruited growth are used (Keith et al. In press). The simulations used herein are based upon the productivity parameters and the non-spatial delay difference model used for the one-year ahead projections.

This research document focuses on the development of limit reference points (LRPs) for SFAs 25A, 26A, 26C, and 27B. Options for the LRPs are developed based on the survey biomass indices, while for the two areas with approved assessment models (SFA 25A and SFA 26A), additional LRPs are developed using the results of maximum sustainable yield (MSY) simulations. In addition to the LRPs, candidate target removal reference (RR_{tar}) and upper stock reference (USRs) points are provided from the MSY simulations. Harvest decision rule (HDR) simulations demonstrate how these simulation techniques can be used, in conjunction with pre-defined management objectives, to inform setting candidate limit removal reference (RR_{lim}) and target reference points (TRPs). This document discusses the concepts of RR_{lim} and RR_{tar}. Herein, RR_{lim} refers to an exploitation rate that should not be exceeded for the stock, whereas RR_{tar} refers to an exploitation rate that the fishery can maintain, on average, over the long-term. The RR_{lim} should always be greater than the RR_{tar}.

In summary, the objectives of this document are:

- To propose and adopt limit reference points for SFAs 25A, 26A, 26C, and 27B; and,

- To provide guidance on upper stock reference points, target reference points, removal reference points, and harvest decision rules.

2. METHODS

2.1. BACKGROUND

The LRPs used throughout this document were derived from estimates of the unfished biomass (B_0) or the biomass at maximum sustainable yield (B_{MSY}, Marentette and Kronlund 2020; DFO 2021, 2023). LRPs typically use 20% of the estimated B_0 ($B_{0(20)}$), 30% of B_{MSY} ($B_{MSY(30)}$), or 40% of B_{MSY} ($B_{MSY(40)}$, DFO 2009, 2021, 2023). For the USR a similar convention is used, herein two USRs are provided for guidance: 40% of B_0 ($B_{0(40)}$) or 80% of B_{MSY} ($B_{MSY(80)}$, DFO 2009; Marentette and Kronlund 2020). In addition to the biomass reference points, guidance on candidate limit (RR_{lim}) and target (RR_{tar}) removal references are provided. For the index based reference points, the biomass indices use the survey index (tonnes) scaled to the survey area and corrected for gear catchability and the removal references are provided as relative indices. The catchability (q) was set at 0.33 for all areas, this is similar to the estimates from both the SFA 25A and SFA 26A models (Keith et al. In press). For consistency between the methods, all analyses used data from 1994 to 2022 inclusive (Keith et al. In press; Keyser et al. In press).

2.2. INDEX BASED METHODS

LRPs and USRs were developed using the survey biomass index time series in four areas (SFA 25A, SFA 26A, SFA 26C, SFA 27B) that are covered by annual surveys. For SFA 26C, a liner was added to the gear in 2008, to increase the catchability of smaller scallop, so the analyses for this area were limited to 2008 onward as changes in the gear can affect selectivity. See Keyser et al. (In press) for more details on the methods underlying the development of the survey biomass indices. The survey biomass indices used to develop the reference points are not corrected for the catchability of the survey gear and the values are not directly comparable to the model based estimates. The survey in SFA 26C is not a stratified survey, thus the area used to estimate the fully-recruited survey biomass index is based on the total area of the survey domain (1,797 km^2).

Survey index based reference points were developed using: 1) the highest three-year geometric mean survey biomass index as a proxy for the stocks carrying capacity or unfished biomass B_0; and, 2) the geometric mean of the time series as a proxy for the biomass at maximum sustainable yield (B_{MSY}). A three-year geometric mean approach was adopted since observation error results in uncertainty around any single year survey biomass estimate and it is challenging to quantify the magnitude of this uncertainty for index based methods. For the three-year geometric mean, the most recent three-years with data is used as the indicator of stock status for a given year; this approach aligns with practices done elsewhere for ascertaining stock status using survey biomass indices (c.f., DFO 2024). In addition, these areas tended to be fished annually, making it possible to utilize the relative exploitation rate index to explore the development of both a RR_{lim} and a RR_{tar}. See Keyser et al. (In press) for more details on the methods underlying the development of the relative exploitation rate index and survey biomass index.

2.2.1. Relative Removal Reference

The four areas noted above tend to be fished annually, making it possible to utilize the relative exploitation rate index to explore the development of both RR_{lim} and RR_{tar}. See Keyser et al. (In

press) for more details on the methods underlying the development of the relative exploitation rate index.

A semi-quantitative method (GEM-Generalized Exploitation Method) that compared the change in the relative survey biomass index (ΔB_r) to the relative exploitation rate (E_r) was used to provide guidance on a candidate RR_{lim} for the index based methods (Jonsen et al. 2009; Sameoto et al. 2024). GEM assumes a linear relationship between the change in the survey index biomass and the relative exploitation rate:

$$\Delta B_{r_i} \sim N\left(0, \sigma_i^2\right)$$
$$E\left(\Delta B_{r_i}\right) = \mu_i$$
$$\mu_i = E_{r_i}$$

where ΔB_r is the expected value of *mu* and is assumed to be normally distributed with a variance of σ^2; *i* represented each observation. A significantly negative slope provides evidence that the fishery has influenced the biomass in the region, and the x-intercept provides an estimate of the relative exploitation rate above which the biomass tends to decline.

A second method was developed to estimate a RR_{tar} for the index based methods. First, the standard deviation of the survey index biomass was calculated using a five-year moving window. For years in which there was no survey data in an area, the survey biomass index was estimated as the mean of the previous and following years' indices (DFO 2022a, 2022b). The five-year period in which the survey biomass index had the lowest standard deviation was selected and the median relative exploitation rate during this period was estimated. This value was provided as an index based candidate RR_{tar}.

2.3. MSY SIMULATIONS

The MSY simulations are undertaken for SFA 25A and SFA 26A using the productivity parameters from the respective stock assessment models for each area. The MSY simulations use the modelled productivity parameters adopted for the one-year ahead projections for the respective areas (Keith et al. In press).

The underlying model for the projection simulations is based on the non-spatial delay difference model used in Keith et al. (In press).

$$B_{fr,t} = e^{-m_{fr,t}} g_{fr,t}\left(B_{fr,(t-1)} - C_{t-1}\right) + e^{-m_{r,t}} g_{r,t} R_{t-1}$$

Fully-recruited biomass is B_{fr}, natural mortality is *m*, growth is *g*, landings are *C*, the recruit biomass is *R*, and the *t* index represents the annual time step, which goes from 1 to the number of years in the simulation. Where applicable, fully-recruited scallops are given the subscript *fr*, while recruits have the subscript *r*. Recruit sized scallop were defined as 75–89 mm (shell height), and fully-recruited scallop were defined as being greater than 90 mm (Keyser et al. In press). In SFA 25A, the fully-recruited growth term ($g_{fr,t}$) parameter is set to one for the simulations, while in SFA 26A the recruit natural mortality (m_r) is the same as the fully-recruited natural mortality (m_{fr}, Keith et al. In press).

2.3.1. Density Dependence

Declines in productivity with increasing adult biomass (i.e., negative density dependence) is thought to be a primary means of population regulation and underpins much of fisheries science (Hilborn and Walters 1992). The relationship between the productivity parameters and the adult biomass (hereafter referred to as spawning stock biomass or SSB) are incorporated into the

population dynamics. Here, it is assumed that the SSB includes both recruit and fully-recruited scallop; as a result, we ignore the potential contribution of scallop with a shell height of less than 75 mm on recruitment. The contribution to recruitment is expected to be minor for scallop under 75 mm in size (Parsons et al. 1992; McGarvey et al. 1993). Evidence for density dependence in the productivity parameters was explored using both quantitative and qualitative methods.

The quantitative method assumed a linear relationship between the productivity parameter and SSB. The linear model structure was:

$$P_i = N(\mu_i, \sigma^2)$$
$$E(P_i) = \mu_i$$
$$\mu_i = \alpha + \beta \times SSB$$

where P_i was the productivity parameter, σ^2 is the variance, μ_i is the expected value of the productivity parameter, α is the intercept, and β is the slope. This was the model used to evaluate density dependence for both the growth and natural mortality productivity terms.

To evaluate density dependence of recruitment, recruitment on a 'per-capita' basis was used as the metric of productivity. The results of the von Bertalanffy analyses suggests that recruit sized scallop in SFA 25A are approximately four years old, while in SFA 26A faster growth results in most recruit size scallop being approximately three years old (Keyser et al. In press). The recruits (*R*) in each SFA were thus offset by three (SFA 26A) or four (SFA 25A) years, respectively, to align with the SSB that produced them (e.g., recruits in SFA 25A in 2022 were assumed to be four years old, thus these scallop were 'born' in 2018, and thus were aligned with the SSB in 2018). The biomass of R was then divided by the SSB in the year the recruits were 'born', giving a recruit per spawner (RPS) metric. When RPS is log transformed and compared to SSB the relationship is a linearization of the Ricker stock-recruit relationship:

$$R_t = \alpha(SSB_t)e^{-\beta(SSB_t)}$$

This can be linearized as:

$$log\left(\frac{R_t}{SSB_t}\right) = \alpha - \beta \times SSB_t$$

thus simplifying to the linear regression formula above with $P = log(\frac{R_t}{SSB_t})$.

This quantitative linear method was initially used to identify evidence for a density dependent relationship (e.g., the blue line with shaded 95% confidence interval in Figure 1). If a density dependent relationship was identified, the linear regression (with uncertainty) was used to account for density dependence in the MSY simulations. However, the predictions from the linear regressions were not used in the MSY simulations because 1) the relationship was rarely linear; and, 2) these linear models could not account for the observed variability in the data and resulted in the parameter estimates (this was particularly problematic for recruitment) having far less variability than observed in the respective stock assessment time series for the productivity parameter. Robust regression techniques were explored to better account for the observed variability, but these techniques did not overcome this challenge.

For this reason, a qualitative visual method was developed to identify the SSB at which a discontinuous non-linear change in a productivity parameter was observed (e.g., the red dashed vertical line in Figure 1). This qualitative method is referred to hereafter as the breakpoint method. Details of how the breakpoints were incorporated into the MSY simulations are described below in the Simulation Procedure section.

2.3.2. Correlation

Autocorrelation in each historically modelled productivity parameter, and cross-correlation between these parameters, were incorporated into the population dynamics for the MSY and HDR simulations. The strength of autocorrelation in these historically modelled productivity parameter was estimated using standard autocorrelation techniques (i.e., the *acf*, *pacf*, and *ccf* functions from the *stats* package in R version 4.2.2, R Core Team 2023). The correlation in RPS was explored on the log scale, while growth and natural mortality were on the natural scale. Where there was evidence for non-stationarity in the respective productivity parameter (e.g., a decline in the parameter estimate over time), the autocorrelation was tested using detrended data (using the residuals from a linear model fit to the productivity time series). There was no evidence of autocorrelation in the growth and most natural mortality parameters; thus, no auto-correlation was modeled for these parameters. The exception was a marginally significant relationship for the fully-recruited natural mortality term for lag 2 in SFA 25A.

2.3.3. Simulation Procedure

In the subsequent text, the 'modelled parameters' refers to parameter estimates from the stock assessment models, these form the basis for our understanding of the historical productivity of each modelled area. The MSY simulations utilize the historical productivity relationships to develop future projections for each stock. In the MSY simulations a single time series projection consists of a user defined number of years, which we refer to as a 'realization'. A 'scenario' combines the results from multiple realizations with a given set of rules (e.g., if a scenario of 10,000 realizations is run with no fishery removals, the results of this would be referred to as a 'no fishing scenario'). The MSY simulations are the result of multiple exploitation rate scenarios using the historical productivity patterns obtained from the stock assessment models.

The MSY simulations build off previous MSY simulation methods developed for scallop stocks in the Maritimes Region, with the current MSY simulations more completely accounting for the variability and correlation between the productivity than previously possible (e.g., Smith et al. 2015). More fully characterizing the productivity dynamics aligns with recommended 'best practices' for the development of reference points (Marentette and Kronlund 2020; Marentette et al. 2021), moreover, these techniques enable the exploration of the impact of more complex harvest strategies on the stock dynamics (see the HDR Simulations section for more details).

The MSY simulations consisted of time series projections of 200 years with 10,000 realizations for each scenario. The scenarios were based on exploitation rates; these exploitation rate scenarios varied the exploitation rate between 0 and 0.1 in steps of 0.005. There was no variability over time in the exploitation rate for a given scenario, e.g., the exploitation rate scenario of 0.1 removed 10% of B_{fr} in every simulated year. The summaries and reference points were calculated using the final 100 years of the projected time series. The results of the density dependence and correlation analyses were used to determine how the productivity parameters would be sampled for these MSY simulations.

The following procedure was applied in cases in which there was no evidence of either density dependence or correlation in the historic modelled productivity parameters. For each productivity parameter, a time series projection with 200 years of parameter values was developed for each of the 10,000 realizations and for each exploitation rate scenario. These time series projections were developed by sampling from a log-normal distribution with the mean (the median for natural mortality as the mean resulted in the simulations having multiple years with fully-recruited natural mortality rates in excess of 90%) and standard deviation taken from the modelled productivity parameter estimates. The log-normal distribution was used to

ensure the productivity parameters remained positive while providing variability in the productivity parameters similar to those historically observed.

When density dependence was observed (i.e., the breakpoint method was used) without correlation, the productivity parameter time series projections were dependent on the SSB estimates and were calculated for each year in each of the projected time series. When a single breakpoint was identified and the simulated SSB for a year was below the breakpoint, the mean (median for *m*) and standard deviation of the historically modelled productivity parameter below the breakpoint were used to sample from a log-normal distribution to obtain a value for the projected productivity parameter for that year. Conversely, when the data were above the breakpoint the same procedure was followed using only data from above the breakpoint SSB. Similarly, if multiple breakpoints were observed (e.g., RPS in SFA 25A), this methodology was followed, using the historical productivity parameters from within the appropriate SSB category.

When correlation was observed in the historically modelled productivity parameters without density dependence, the productivity parameter time series projection used the historical time series auto-correlation with the mean (median for *m*) and standard deviation of the time series projection set based on the historical productivity parameter. Auto-correlation was incorporated using an auto-regressive integrated moving average (ARIMA) framework (i.e., using the *arima.sim* function from the *stats* package, and the *rmvnorm* function from the *mvtnorm* package, R version 4.2.2, R Core Team 2023), using the first two auto-regressive components.

Where correlation and density dependence were both found in a historical productivity parameter(s), both of these characteristics were incorporated into the productivity parameter time series projections. The first step was to develop the productivity parameter time series projection with the auto- and cross-correlation structure observed in the historical productivity parameter time series using the above ARIMA methods. Additionally, the mean (median for *m*) and standard deviation of the projected time series was set based on the historical productivity parameter estimates from below the breakpoint SSB (historically there are more years in which the stock was below the breakpoint). The second step was to update the productivity parameter estimate in the time series projection in years that SSB was above the breakpoint. In this step, the productivity parameter estimate for the year was replaced by a sample from a log-normal distribution with a mean and standard deviation estimated from the historical productivity parameter above the breakpoint. This procedure somewhat weakened the strength of the correlation in the time series projections, but resulted in time series in which the general correlation structure and density dependence relationships of the original productivity time series were retained (see the Results section).

Cross-correlation was only observed between the RPS and fully-recruited natural mortality productivity parameters. This cross-correlation may be related to the challenges that have been observed with delay difference models independently estimating values of both parameters (e.g., McDonald et al. 2021). The cross-correlation analysis was used to identify the peak correlation at time lags of less than five years between these two parameters using the historical productivity of RPS and fully-recruited natural mortality. The time series projections were developed using an ARIMA framework to simulate RPS and natural mortality time series to retain the characteristics of the observed RPS and natural mortality time series. Density dependence in RPS was incorporated into the time series projection as described in the previous paragraph.

Finally, to constrain the MSY simulations from reaching unrealistically high biomass estimates, whenever the SSB exceeded the maximum observed SSB in the historical modelled time series, the fully-recruited growth parameter was set to 1 and sampled from a log-normal distribution with a standard deviation of 0.1.

2.3.4. Model Derived Indices

B_{MSY} and B_0 were estimated from the MSY simulation results. B_0 was calculated as median biomass of the final 100 years from the simulations in which the exploitation rate was set to zero. B_{MSY} was calculated as the median biomass of the final 100 years of the simulations using the exploitation rate that resulted in the average yield from the fishery being maximized (MSY) using the final 100 years of simulated data. The exploitation rate at B_{MSY} was the long-term target exploitation rate and this can be used to inform the setting of the RR_{tar}.

As with the index based methods, the criteria for the proposed LRPs and suggested USRs were based on B_0 and B_{MSY}. Proposed LRPs were set at 20% of B_0 ($B_{0(20)}$) and 30% ($B_{MSY(30)}$) and 40% ($B_{MSY(40)}$) of B_{MSY}, while candidate USRs at 40% of B_0 ($B_{0(40)}$) and at 80% of B_{MSY} ($B_{MSY(80)}$) were provided. An additional benefit of using stochastic simulations is the ability to identify the percentage of the years in which the stocks were in the critical (below the LRP), cautious (between the LRP and USR), and healthy zones (above the USR). Using the final 100 years of data, $B_{0(20)}$ as the LRP, and $B_{0(40)}$ as the USR, the proportion of the time each of the simulations were in these zones from the scenario in which fishing at the exploitation rate that resulted in the biomass being at B_{MSY}.

2.4. HDR SIMULATIONS

The stochastic simulations developed herein can be used to explore scenarios that utilize more complex harvest strategies than explored in the above MSY simulations (where the exploitation rate for each scenario is fixed through time). For the HDR simulations, the productivity parameters are simulated as per the above procedures, but instead of using a fixed exploitation rate for a scenario, it can be varied as a function of the current simulated biomass. In addition, HDR scenarios can be developed that link the exploitation rates to the reference points and explore how varying the exploitation rates at each of the reference points (often referred to as control points) will impact the stock dynamics over the long-term.

While these HDR simulations are not required for setting the LRP, an exploration of different HDR scenarios provide additional understanding of the impact of implementing different USRs and RR_{tar}. Additionally, these HDR simulations enable the exploration of additional reference points, such as the development of a biomass based target reference point (TRP) and a limit removal reference (RR_{lim}; DFO 2009, Marentette and Kronlund 2020). The TRP is a value above the USR and is determined by productivity objectives or other biological considerations (Marentette and Kronlund 2020, DFO 2021, 2023).

There are innumerable HDR scenarios that could be tested, but scenarios should be designed to address management objectives. The HDR simulations have the potential to inform alternative harvesting strategies that could support both conservation and socioeconomic objectives. The code to explore the impact of various HDR scenarios on the stock is publicly available (Keith 2025). Defining HDRs is not the purview of Science and there are no established HDRs for the SFAs evaluated here; however, we present a HDR scenario for each of SFA 25A and SFA 26A to demonstrate the utility of this approach.

For the HDR scenarios, the management objectives were to a) maintain the stock near the TRP, b) increase the long term average removals from the fishery, and c) reduce the percentage of the years that the stock was below the LRP. The HDR scenario results for objectives b) and c) were compared to the results from the MSY simulations scenario in which the exploitation rate resulted in the population being at B_{MSY}. In each HDR scenario, the TRP was set at the B_{MSY} estimate, the LRP was set at $B_{MSY(40)}$, and the USR was set at $B_{MSY(80)}$. The mean exploitation rate was set as described below. A log-normal distribution with standard deviation of 0.1 was used to allow for some variability in the exploitation rate. These results summarize the final 100

years of the 10,000 realizations and, similar to the MSY simulations, the percentage of the years in which the results are observed to be below the LRP, above the USR, above the TRP, or between these reference points was calculated.

In SFA 25A, the HDR scenario set the exploitation rate to a) a RR_{lim} of 0.05 when when B_{fr} was above the TRP (2,900 tonnes), b) 0.02 when B_{fr} was above the USR (2,320 tonnes) but below the TRP, c) decline linearly from 0.02 at the USR, to 0 at the LRP (1,160 tonnes) when B_{fr} was below the USR but above the LRP , d) 0 when B_{fr} was below the LRP. Similarly, in SFA 26A, the HDR scenario set the exploitation rate to a) an RR_{lim} of 0.07 when B_{fr} was above the TRP (5,000 tonnes), b) 0.03 when B_{fr} was above the USR (4,000 tonnes) and below the TRP, c) decline linearly from 0.03 at the USR, to 0 at the LRP (2,000 tonnes) when B_{fr} was below the USR but above the LRP, d) 0 when B_{fr} was below the LRP.

3. RESULTS

3.1. PRODUCTIVITY AND DENSITY DEPENDENCE

3.1.1. SFA 25A

There was clear evidence for negative density dependence in recruitment; RPS increased as biomass declined (Figure 1). The general relationship followed the expectation of a Ricker model (Figure 1), but as noted above, the breakpoint method was preferred for use in the MSY simulations. The breakpoint used was 7,000 tonnes (Figure 1). A second potential breakpoint was identified at 4,300 tonnes, however simulation testing using this additional breakpoint lead to the stock consistently producing relatively large recruit biomass whenever the stock biomass was below 4,300 tonnes. This resulted in the simulations using this breakpoint supporting exploitation rates that were two to three times higher than has ever been observed in SFA 25A. As a result this additional breakpoint was not incorporated into the simulations. There was no evidence for density dependence in the growth or natural mortality parameters (Figures 2 and 3). There were also no discontinuous breaks in the relationships between growth or natural mortality as SSB increased (Figures 2 and 3). Therefore, no density dependence was incorporated into the MSY or HDR simulations for the growth or natural mortality parameters.

There was evidence of autocorrelation in the RPS time series, with a significant positive correlation (0.68) at a one year lag (Figure 4). There was no evidence of correlation in the growth parameters (Figure 5). A weakly significant negative correlation (-0.38) was observed at a two year lag for the fully-recruited mortality and this was incorporated into the simulations, while there was no correlation in the recruit mortality time series (Figure 6). Finally, the cross-correlation between RPS (offset to the year the recruits are observed in the time series) and fully-recruited natural mortality was evaluated and a weak but significant correlation was observed in the relationship. The highest correlations were observed between lags of -1 to 1 years, with the peak at 1 (r=0.46, Figure 7). This suggests that relatively large recruit biomass events (given the SSB that produced the recruits) were observed during periods of high natural mortality. Alternatively, relatively small recruit biomass events were observed during periods of high natural mortality. To account for this effect, the simulations included the correlation between fully-recruited natural mortality and RPS at the peak lag.

The annual survey biomass index estimates were highly correlated (r=0.98) to the model biomass estimates, although there were several years in which the survey biomass index was noticeably different than the resultant model biomass estimate (e.g., 1995, 2010, and 2022) and most of the data fell near the 1:1 line (Figure 8). This indicated that the survey biomass index

was generally a reasonable proxy for the model biomass, but the two metrics will differ when comparing individual years (Figure 8).

3.1.2. SFA 26A

There was clear evidence for negative density dependence in recruitment, RPS increased as biomass declined (Figure 9). The general relationship followed the expectation of a Ricker model (Figure 9), but as noted above, the breakpoint method was preferred for use in the MSY simulations. A single breakpoint was identified, when the SSB was above 11,500 tonnes RPS tended to be the lowest observed in the time series, while there was no evidence for a trend in RPS with changes in SSB below this value (Figure 9). There was little evidence for density dependence in the growth or natural mortality parameters (Figures 10 and 11). There were also no discontinuous breaks in the relationships between growth and SSB (Figure 10), although we note that low values of natural mortality were not observed when the SSB was above approximately 13,000 tonnes (Figure 11). As a result, no density dependence was incorporated into the MSY or HDR simulations for growth or natural mortality.

There was evidence of autocorrelation in the RPS time series, with a significant positive correlation (0.7) at a one year lag and a significant negative correlation at a two year lag (-0.61, Figure 12). There was no significant correlation in the growth or natural mortality time series (Figures 13 and 14). Finally, the cross-correlation between RPS (offset to the year the recruits are observed in the time series) and fully-recruited natural mortality was evaluated. A significant correlation was observed in the relationship; the highest correlations were observed between lags of 0 to 2 years, with the peak at a lag of -1 year (r=0.77, Figure 15). This suggests that relatively large recruit biomass events (given the SSB that produced the recruits) were observed during periods of high natural mortality. Alternatively, relatively small recruit biomass events were observed during periods of high natural mortality. To account for this effect, the simulations included the correlation between fully-recruited natural mortality and RPS at the peak lag.

The annual survey biomass index estimates were correlated (r=0.76) to the model biomass estimates, although the survey biomass index does not follow the model biomass estimates as closely as observed in SFA 25A (Figure 16). In several of the early years in the time series (i.e., 1994-1998), the model biomass estimate is notably higher than the survey biomass index. This may be related to the initial conditions required for SEAM (Keith et al. In press). In general, these results indicated that the survey biomass index is a reasonable proxy for the model biomass, especially in more recent years, but that differences between the two metrics in a particular year can be substantial (Figure 16).

3.2. REFERENCE POINTS

3.2.1. Survey Biomass Indices

Three survey biomass index based LRPs were developed for each area (Table 1). In SFA 25A the three LRPs were, 1,255 tonnes ($B_{MSY(30)}$), 1,674 tonnes ($B_{MSY(40)}$), and 1,338 tonnes ($B_{0(20)}$; Figure 17). In SFA 26A the three LRPs were 1,913 tonnes ($B_{MSY(30)}$), 2,551 tonnes ($B_{MSY(40)}$), and 3,252 tonnes ($B_{0(20)}$; Figure 17). In SFA 26C the three LRPs were, 890 tonnes ($B_{MSY(30)}$), 1,187 tonnes ($B_{MSY(40)}$), and 882 tonnes ($B_{0(20)}$; Figure 17). In SFA 27B the three LRPs were, 628 tonnes ($B_{MSY(30)}$), 837 tonnes ($B_{MSY(40)}$), and 771 tonnes ($B_{0(20)}$; Figure 17).

Two survey biomass index based candidate USRs were developed in each area (Table 1). In SFA 25A the two USRs were, 3,347 tonnes ($B_{MSY(80)}$) and 2,676 tonnes ($B_{0(40)}$; Figure 17). In SFA 26A the two USRs were, 5,102 tonnes ($B_{MSY(80)}$) and 6,503 tonnes ($B_{0(40)}$; Figure 17). In

SFA 26C the two USRs were, 2,373 tonnes ($B_{MSY(80)}$) and 1,763 tonnes ($B_{0(40)}$; Figure 17. In SFA 27B the two USRs were, 1,674 tonnes ($B_{MSY(80)}$) and 1,542 tonnes ($B_{0(40)}$; Figure 17).

Phase plots using the relative removal and survey biomass indices indicated that the relative exploitation rate did not have a clear relationship to the survey biomass index in any of the areas (Figure 18). GEM was unable to identify a relationship between the change in biomass indices and relative exploitation rate in SFA 25A, 26C, or 27B that would facilitate the development of a RR_{lim} in these areas (Figure 19). In SFA 26A, the change in the biomass index tended to decline as the relative exploitation rate increased which facilitated the development of a candidate RR_{lim} using the relative indices; the GEM suggested a candidate RR_{lim} of approximately 0.12 (top right panel, Figure 19 and Table 1).

A candidate relative RR_{tar} was identified in each of the areas as the median relative exploitation rate of the five-year period with the least variability in the survey biomass index (Table 1). In SFA 25A, the candidate relative RR_{tar} was 0.011 based on the relative exploitation rate between 2011 and 2015. In SFA 26A, the candidate relative RR_{tar} was 0.077 based on the relative exploitation rate between 2018 and 2022. In SFA 26C, the candidate relative RR_{tar} was 0.025 based on the relative exploitation rate between 2015 and 2019. In SFA 27B, the candidate relative RR_{tar} was 0.15 based on the relative exploitation rate between 2002 and 2006.

3.2.2. MSY Simulations

In SFA 25A, the MSY simulation time series projections of the productivity parameters had similar characteristics to historically modelled time series. The time series projections from the MSY scenario in which the exploitation rate was set to 0.03 were compared to the historically modelled time series. The recruit growth and natural mortality parameters from the simulations had minimal auto-correlation (Figure 20). The simulated RPS time series retained the lag 1 correlation without any notable lag 2 correlation (mean simulation estimates were 0.64 and -0.01 respectively, Figure 20). The fully-recruited natural mortality retained the lag 2 correlation without any notable lag 1 correlation (mean simulation estimate were -0.35 and -0.01 respectively, Figure 20). In addition, the peak correlation between natural mortality and RPS was also present in the simulated data at lag 1; however, as with the RPS and natural mortality auto-correlation, this value was somewhat lower in the simulations (the mean simulation estimate was 0.24, Figure 21). The density dependence observed in the RPS data was retained in the simulations, with recruitment being consistently low when the SSB exceeded the SFA 25A breakpoint (7,000 tonnes) and the RPS values below the breakpoint were similar to the underlying observed RPS values, no density dependence was observed in the other simulated productivity parameters (Figure 22).

In SFA 25A, the MSY simulation results indicated that the median biomass stabilized at approximately 4,700 tonnes when the exploitation rate was 0 (Figure 23). This is hereafter considered the unfished biomass (B_0) for SFA 25A. The exploitation rate that maximized the removals in the long term was 0.03 (Figure 24); this was considered a candidate RR_{tar} for SFA 25A based on the historically observed productivity regime. The median biomass at this RR_{tar} was 2,900 tonnes and this was considered the biomass at maximum sustainable yield (B_{MSY}; Figure 25). The median annual removals at B_{MSY} were 88 tonnes (Figure 24).

Based on these values, three MSY simulation based LRPs were proposed for SFA 25A, 870 tonnes ($B_{MSY(30)}$), 1,160 tonnes ($B_{MSY(40)}$), and 940 tonnes ($B_{0(20)}$; Figure 26 and Table 2). Two MSY simulation candidate USRs were provided for SFA 25A, 2,320 tonnes ($B_{MSY(80)}$) and 1,880 tonnes ($B_{0(40)}$; Figure 26 and Table 2). Using the MSY scenario with the exploitation rate of 0.03, and with a LRP set at $B_{MSY(40)}$ and a USR of $B_{MSY(80)}$ as examples, the simulations for SFA 25A resulted in the population being above the USR (i.e., in the healthy zone) in 64.1% of the

simulated years, below the LRP (i.e., in the critical zone) in 9.3% of the simulated years, and between the LRP and USR (i.e., in the cautious zone) in 26.6% of the simulated years (Figure 27).

In SFA 26A, the MSY simulation time series projections of the productivity parameters had similar characteristics to historically modelled productivity time series. The time series projections from the MSY scenario in which the exploitation rate was set to 0.04 were compared to the historically modelled productivity time series. The growth and natural mortality parameters from the simulations had minimal auto-correlation (Figure 28). The simulated RPS time series retained both a lag 1 and lag 2 correlation (mean simulation estimates were 0.4 and -0.42 respectively; this correlation was somewhat weaker than the observed RPS time series, Figure 28). In addition, the peak correlation between natural mortality and RPS was also present in the simulated data at lag -1, however as with the RPS and natural mortality auto-correlation, this value was somewhat lower in the simulations (the mean simulation estimate was 0.47, Figure 29). The density dependence of RPS was retained, with it being consistently low when the SSB exceeded the SFA 26A breakpoint (11,500 tonnes) and the value of RPS below the breakpoint being similar to the underlying observed RPS values, no density dependence was observed in the other simulated productivity parameters (Figure 30).

In SFA 26A, the MSY simulation results indicated that the median biomass stabilized at approximately 8,300 tonnes when the exploitation rate was 0 (Figure 31). This is hereafter considered the unfished biomass (B_0) for SFA 26A. The exploitation rate that maximized the removals in the long term was 0.04 (Figure 32), this was considered a candidate RR_{tar} for SFA 26A based on the historically observed productivity regime. The median biomass at the RR_{tar} was 5,000 tonnes and this was considered the biomass as maximum sustainable yield (B_{MSY}; Figure 33). The median annual removals at B_{MSY} were 200 tonnes (Figure 32).

Based on these values three MSY simulation based LRPs are proposed for SFA 26A, 1,500 tonnes ($B_{MSY(30)}$), 2,000 tonnes ($B_{MSY(40)}$), and 1,660 tonnes ($B_{0(20)}$; Figure 34 and Table 2). Two MSY simulation candidate USRs are provided for SFA 26A, 4,000 tonnes ($B_{MSY(80)}$) and 3,320 tonnes ($B_{0(40)}$; Figure 34 and Table 2). Using the MSY scenario with the exploitation rate of 0.04, and with a LRP set at $B_{MSY(40)}$ and a USR of $B_{MSY(80)}$ as examples, the simulations for SFA 26A resulted in the population being above the USR (i.e., in the healthy zone) in 63% of the simulated years, below the LRP (i.e., in the critical zone) in 13.5% of the simulated years, and between the LRP and USR (i.e., in the cautious zone) in 23.5% of the simulated years (Figure 35).

3.3. HDR SIMULATIONS

For the SFA 25A HDR scenario, the median biomass (2,878 tonnes) fluctuated around the TRP (Figure 36). The average removals were 119 tonnes, while the median removals were 64 tonnes (Figure 37). The stock was below the LRP in 2.37% of the simulated years, in the cautious zone in 27.6% of the simulated years, between the USR and the TRP in 20.7% of the simulated years, and above the TRP in 49.2% of the simulated years (Figure 38). This results in a bifurcation of the landings; for example, while the stock is above the USR but below the TRP, landings generally ranged from 46.4 to 58 tonnes, while above the TRP the landings were usually greater than 145 tonnes, and occasionally were more than double this (Figure 39).

For the SFA 26A HDR scenario, the median biomass (4,913 tonnes) fluctuated around the TRP (Figure 40). The mean removals were 281 tonnes, while the median removals were 159 tonnes (Figure 41). The stock was below the LRP in 2% of the simulated years, it was in the cautious zone in 27.7% of the simulated years, it was between the USR and the TRP in 22.2% of the simulated years, and was above the TRP in 48.1% of the simulated years (Figure 42). This

results in a bifurcation of the landings; for example, while the stock is above the USR but below the TRP, landings generally ranged from 120 to 150 tonnes, while above the TRP the landings were usually greater than 350 tonnes, and occasionally were more than double this (Figure 43).

4. CONCLUSIONS

Information to guide the development of USRs, TRPs, and RRs has been provided for each of the four areas (SFAs 25A, 26A, 26C, and 27B). For all areas, the B_{MSY} reference points were preferred given the challenges of estimating B_0 for stocks with an active fishery. In areas with both model based and index based reference points (SFA 25A and SFA 26A), the model based reference points were deemed to be more informative. In both modeled areas $B_{MSY(40)}$ was preferred as the LRP as it most closely aligned with the principles of the precautionary approach. For the modeled areas, the exploration of the HDR scenarios in this document were example based; further development of this approach could take into account established or potential future management objectives.

For the areas with only index based reference points (SFAs 26C and 27B) $B_{MSY(30)}$ was recommended as the LRP. This LRP was chosen because the index based reference points were more precautionary in nature (closer to the minimum observed value in the time series) than the corresponding model based reference points in areas where both sets of reference points were available. The index based methods developed to identify potential RRs were unable to disentangle environmental and fishery impacts on the stock and were not recommended to be used to determine the RR for the index based areas. Finally, it is not recommended to implement both USRs and TRPs for the survey index based RPs as the potential for increased removals and a decrease in the probability of being below the LRP result from the additional HDRs being set around the TRP; development of these HDRs would be challenging given the data constraints associated with the survey index based based RPs.

The MSY simulations identified three candidate model based LRPs for SFA 25A, 940 tonnes ($B_{0(20)}$), 870 tonnes ($B_{MSY(30)}$), and 1,160 tonnes ($B_{MSY(40)}$). These simulations were also used to identify two candidate model based USRs, 1,880 tonnes ($B_{0(40)}$) and 2,320 tonnes ($B_{MSY(80)}$), along with a candidate RR_{tar} of 0.03. The $B_{MSY(40)}$ (1,160 tonnes) LRP was adopted for SFA 25A.

The MSY simulations identified three candidate model based LRPs for SFA 26A, 1,660 tonnes (20% of B_0), 1,500 tonnes (30% of B_{MSY}), and 2,000 tonnes ($B_{MSY(40)}$). These simulations were also used to identify two candidate model based USRs, 3,320 tonnes ($B_{0(40)}$) and 4,000 tonnes ($B_{MSY(80)}$), along with a candidate RR_{tar} of 0.04. The $B_{MSY(40)}$ (2,000 tonnes) LRP was adopted for SFA 26A.

For SFA 26C, three survey index based LRPs were proposed, 882 tonnes ($B_{0(20)}$), 890 tonnes ($B_{MSY(30)}$), and 1,187 tonnes ($B_{MSY(40)}$). Using the survey index based methods in SFA 26C, guidance for two USRs was provided, 1,763 tonnes ($B_{0(40)}$) and 2,373 tonnes ($B_{MSY(80)}$). There was no consistent relationship observed between biomass change and the relative exploitation rate, and thus the GEM method was unable to provide guidance for a RR_{lim}. A candidate RR_{tar} value of 0.025 was identified using the median relative exploitation rate during the five-year period with the least biomass variability observed in the survey biomass index; during these five years growth and recruitment were typical for the area, although we note this is the shortest time series available in this analysis (Keyser et al. In press). The $B_{MSY(30)}$ (890 tonnes) LRP was adopted for SFA 26C.

For SFA 27B, three survey index based LRPs were proposed, 771 tonnes ($B_{0(20)}$), 628 tonnes ($B_{MSY(30)}$), and 837 tonnes ($B_{MSY(40)}$). Using the survey index based methods in SFA 27B, guidance for two USRs was provided, 1,542 tonnes ($B_{0(40)}$) and 1,674 tonnes ($B_{MSY(80)}$). There

was no consistent relationship observed between biomass change and the relative exploitation rate, and thus the GEM method was unable to provide guidance for a RR_{lim}. A candidate RR_{tar} value of 0.15 was identified using the median relative exploitation rate during the five-year period with the least biomass variability observed in the survey biomass index; during these five years growth was typical for the area, while recruitment was above average (Keyser et al. In press). The $B_{MSY(30)}$ (628 tonnes) LRP was adopted for SFA 27B.

In case the model biomass estimates are unavailable for a model based area, the utility of using the survey biomass indices as a proxy for the stock status was also explored for the two modelled areas. In SFA 25A, the survey biomass index is highly correlated to the model biomass estimate, so the survey biomass can be used to infer stock status. In SFA 26A, while the survey index is somewhat correlated to the model biomass estimate, the differences between the two metrics can be substantial and caution is recommended if attempting to the survey biomass index as a proxy for the biomass.

The HDR scenarios were used to highlight how this approach can be used to identify candidate RR_{lim} and TRPs for the modelled areas. In both areas, the HDR scenario used reduced the probability of the stock declining below the LRP and increased the long-term average harvest levels when compared to the MSY simulation scenario that resulted in B_{MSY}. This adaptive strategy accomplished this by reducing the exploitation rate in the healthy zone below the exploitation rate at B_{MSY} (which is commonly used as either the RR_{lim} or RR_{tar}), while allowing removals to exceed the exploitation rate at B_{MSY} when the biomass was above the TRP. Within the context of the DFO precautionary approach the RR_{lim} identified in these HDR simulations could serve as the maximum allowable exploitation rate which would only be applicable when the stock is above its TRP (DFO 2021, 2023). The HDR scenarios lead to much higher inter-annual variability in removals, with relatively large removals occurring approximately 50% of the time, but relatively low removals in the near term as the biomass increases towards the TRP. However, the maximum removals that would be recommended when the stocks are above the USR but below the TRP are higher than the removals in recent years in SFA 25A, and similar to the recent removals in SFA 26A. Finally, more complex HDRs could be explored, such as allowing the RR_{lim} to be a function of the biomass whenever the biomass is above a TRP.

The models in SFA 25A and 26A should be subject to re-evaluation to ensure they continue to capture the population dynamics of the areas, and to monitor for changes in the productivity of each stock. It is challenging to predict when the models should next be re-evaluated as this is a function of ecological, social, and economic factors which cannot be forecast. It is recommended to monitor the growth, RPS, natural mortality, and process error components of the models. A long-term directional bias in the growth, RPS, natural mortality, or process error would indicate a shift in the productivity of the stock. This would indicate the need for additional research to understand the processes driving the changes and may enable the development of models that attempt to account for the changes in productivity. Such a productivity shift would also impact the reference points for the area and would require additional simulation testing.

The methods used here relied on fishery-independent metrics (i.e., model output or survey indices). While reference points can be developed using fishery-dependent data, fishery-dependent methods would not be appropriate for these areas because of the rapid increase in fishery efficiency over the last two decades and the adoption of larger more powerful vessels over the last 30 years (Keith et al. 2020; Keyser et al. In press). Fishery dependent methods generally rely on using some measure of catch per unit effort (CPUE), with the underlying assumption that CPUE is proportional to the biomass of the population (Hilborn and Walters 1992). However, when changes in fishing efficiency are driven by technological or behavioral changes, CPUE is not proportional to the population biomass, and this assumption is invalid.

Using fishery-dependent methods in this context would result in a biased understanding of stock status that would result in biased science advice.

5. RESEARCH RECOMMENDATIONS

There is substantial spatial and temporal (both intra- and inter-annual) variability in both growth and condition of scallop. Additional research to enhance our understanding of this variability, its causes, and the impact on the fishery and our understanding of stock status was a primary recommendation from this process. Research has begun to start to quantify this variability for Georges Bank using available port sampling data and new ageing data (see Keyser et al. in Prep for details of the port sampling data), however additional research will be necessary to better capture the impacts of this variability across the offshore areas.

For areas using index based reference points, challenges with identifying appropriate RR using the methods developed herein were noted. A general recommendation was to explore alternative methods to define the RR for the index based areas and to explore additional methods to estimate biomass based reference points (e.g., yield per recruit modelling) in these areas. A major challenge with the RR methods used was the inability of the methods to disentangle the importance of environmental and fishery effects on population change, future methods should attempt to overcome this limitation.

Understanding connectivity between these populations and with adjacent populations in other jurisdictions would enhance our understanding of the population dynamics, especially with respect to recruitment variability. Knowledge of connectivity of sea scallop stocks within the Northwest Atlantic is an active area of research (Wyngaarden et al. 2017; Chen et al. 2021; Economou et al. 2024). Continued research into this will enable the development of more advanced stock-recruitment models and enhance our understanding of the population dynamics of these stocks.

REFERENCES CITED

Chen, C., Zhao, L., Gallager, S., Ji, R., He, P., Davis, C., Beardsley, R.C., Hart, D., Gentleman, W.C., Wang, L., Li, S., Lin, H., Stokesbury, K., and Bethoney, D. 2021. Impact of larval behaviors on dispersal and connectivity of sea scallop larvae over the northeast U.S. Shelf. Progress in Oceanography 195: 102604.

DFO. 2009. A fishery decision-making framework incorporating the precautionary approach.

DFO. 2021. Science Advice for Precautionary Approach Harvest Strategies under the Fish Stocks Provision.

DFO. 2022. Stock Status Update for Scallop (*Placopecten magellanicus*) in Scallop Fishing Area 29 West of Longitude 65°30'. DFO Can. Sci. Advis. Sec. Sci. Resp. 2022/042.

DFO. 2022. Stock Status Update of Browns Bank North Scallops (*Placopecten magellanicus*) for the 2022 Fishing Season. DFO Can. Sci. Advis. Sec. Sci. Resp. 2022/037.

DFO. 2023. Science Advice on Guidance for Limit Reference Points under the Fish Stocks Provisions.

DFO. 2024. Maritimes Research Vessel Survey Trends on the Scotian Shelf and Bay of Fundy for 2023. DFO Can. Sci. Advis. Sec. Sci. Resp. 2024/010.

Economou, K.N., Gentleman, W.C., Krumhansl, K.A., DiBacco, C., Reijnders, D., Wang, Z., Lyons, D.A., and Lowen, B. 2024. Assessing spatial structure in marine populations using network theory: A case study of Atlantic sea scallop (Placopecten magellanicus) connectivity. PLOS ONE 19(11): e0308787. Public Library of Science.

Hilborn, R., and Walters, C.J. 1992. Quantitative fisheries stock assessment: Choice, dynamics and uncertainty. Chapman and Hall, New York.

Jonsen, I.D., Glass, A., Hubley, B., and Sameoto, J. 2009. Georges Bank 'a' scallop (*Placopecten Magellanicus*) framework assessment: Data inputs and population models. DFO Can. Sci. Advis. Sec. Res. Doc. 2009/034: iv + 76 p.

Keith, D.M. 2025. Offshore Scallop Harvest Decision Rule Simulations.

Keith, D.M., Keyser, F.M., McDonald, R., Pearo Drew, T., and Sameoto, J.A. In press. Framework Development for Scallop Fishing Areas 25a, 25b, 26a, 26b, 26c, and 27b: Stock Assessment Models for SFAs 25 and 26. DFO Can. Sci. Advis. Sec. Res. Doc.

Keith, D.M., Sameoto, J.A., Keyser, F.M., and Ward-Paige, C.A. 2020. Evaluating socio-economic and conservation impacts of management: A case study of time-area closures on Georges Bank. PLOS ONE 15(10): e0240322.

Keyser, F.M., Glass, A., Keith, D.M., McDonald, R.R., Pearo Drew, T., and Sameoto, J.A. In press. Framework Development for Scallop Fishing Areas 25a, 25b, 26a, 26b, 26c, and 27b: Data Inputs. DFO Can. Sci. Advis. Sec. Res. Doc.

Marentette, J.R., and Kronlund, R.A. 2020. A Cross-Jurisdictional Review of International Fisheries Policies, Standards and Guidelines: Considerations for a Canadian Science Sector Approach. Can. Tech. Rep. Fish. Aquat. Sci. 3342.

Marentette, J.R., Kronlund, R.A., and Cogliati, K.M. 2021. Specification of Precautionary Approach Reference Points and Harvest Control Rules in Domestically Managed and Assessed Key Harvested Stocks In Canada.

McDonald, R.R., Keith, D.M., Sameoto, J.A., Hutchings, J.A., and Flemming, J.M. 2021. Explicit incorporation of spatial variability in a biomass dynamics assessment model. ICES Journal of Marine Science.

McGarvey, R., Serchuk, F.M., and McLaren, I.A. 1993. Spatial and Parent-Age Analysis of Stock–Recruitment in the Georges Bank Sea Scallop (Placopecten magellanicus) Population. Can. J. Fish. Aquat. Sci. 50(3): 564–574. NRC Research Press.

Parsons, G., Robinson, S., Chandler, R., Davidson, L., Lanteigne, M., and Dadswell, M. 1992. Intra-annual and long-term patterns in the reproductive cycle of giant scallops Placopecten magellanicus (Bivalvia: Pectinidae) from Passamaquoddy Bay, New Brunswick, Canada. Mar. Ecol. Prog. Ser. 80: 203–214.

R Core Team. 2023. R: A language and environment for statistical computing. R Foundation for Statistical Computing, Vienna, Austria.

Sameoto, J.A., Keyser, F.M., and Keith, D.M. 2024. Assessing the Productivity of the Scallop Stocks in Scallop Production Areas in the Bay of Fundy and Scallop Fishing Area 29W and the Impact of Two-Year Projection Advice. DFO Can. Sci. Advis. Sec. Res. Doc. 2024/065. iv + 108 p.

Smith, S.J., Nasmith, L., Glass, A., Hubley, B., and Sameoto, J. 2015. Framework assessment for SFA 29 West scallop fishery. DFO Can. Sci. Advis. Sec. Res. Doc. 2014/110: v + 69 p.

Wyngaarden, M.V., Snelgrove, P.V.R., DiBacco, C., Hamilton, L.C., Rodríguez-Ezpeleta, N., Jeffery, N.W., Stanley, R.R.E., and Bradbury, I.R. 2017. Identifying patterns of dispersal, connectivity and selection in the sea scallop, *Placopecten Magellanicus, Using RADseq-derived SNPs*. Evolutionary Applications 10(1): 102–117.

TABLES

Table 1. A summary of the reference points for each area calculated using the survey index based methods. The LRPs include, 30% of the median survey biomass index ($B_{MSY(30)}$), 40% of the median survey biomass index ($B_{MSY(40)}$), and 20% of the maximum survey biomass index ($B_{0(20)}$). The USRs include, 80% of the median survey biomass index ($B_{MSY(80)}$) and 40% of the maximum survey biomass index ($B_{0(40)}$). The limit removal reference (RR_{lim}) was calculated using the GEM method, while the target removal reference (RR_{tar}) was the median removals during the five-year period of time in which the survey biomass index had the least variability. The survey biomass indices were catchability corrected using a

	$B_{MSY(30)}$	$B_{MSY(40)}$	$B_{0(20)}$	$B_{MSY(80)}$	$B_{0(40)}$	RR_{lim}	RR_{tar}
SFA 25A	1,255	1,674	1,338	3,347	2,676	NA	0.011
SFA 26A	1,913	2,551	3,252	5,102	6,503	0.12	0.077
SFA 26C	890	1,187	882	2,373	1,763	NA	0.025
SFA 27B	628	837	771	1,674	1,542	NA	0.150

Table 2. A summary of the reference points for SFA 25A and SFA 26A calculated using the MSY simulations. The LRPs include, 30% of the median biomass at the simulation estimate of maximum sustainable yield ($B_{MSY(30)}$), 40% of the median biomass at the simulation estimate of maximum sustainable yield ($B_{MSY(40)}$), and 20% of the median biomass using simulations with no fishing ($B_{0(20)}$). The USRs include, 80% of the median biomass at the simulation estimate of maximum sustainable yield ($B_{MSY(80)}$) and 40% of the median biomass using simulations with no fishing ($B_{0(40)}$). The target removal reference (RR_{tar}) was calculated as the exploitation rate which resulted in the maximum sustainable yield.

	$B_{MSY(30)}$	$B_{MSY(40)}$	$B_{0(20)}$	$B_{MSY(80)}$	$B_{0(40)}$	RR_{tar}
SFA 25A	870	1,160	940	2320	1880	0.03
SFA 26A	1,500	2,000	1,660	4000	3320	0.04

FIGURES

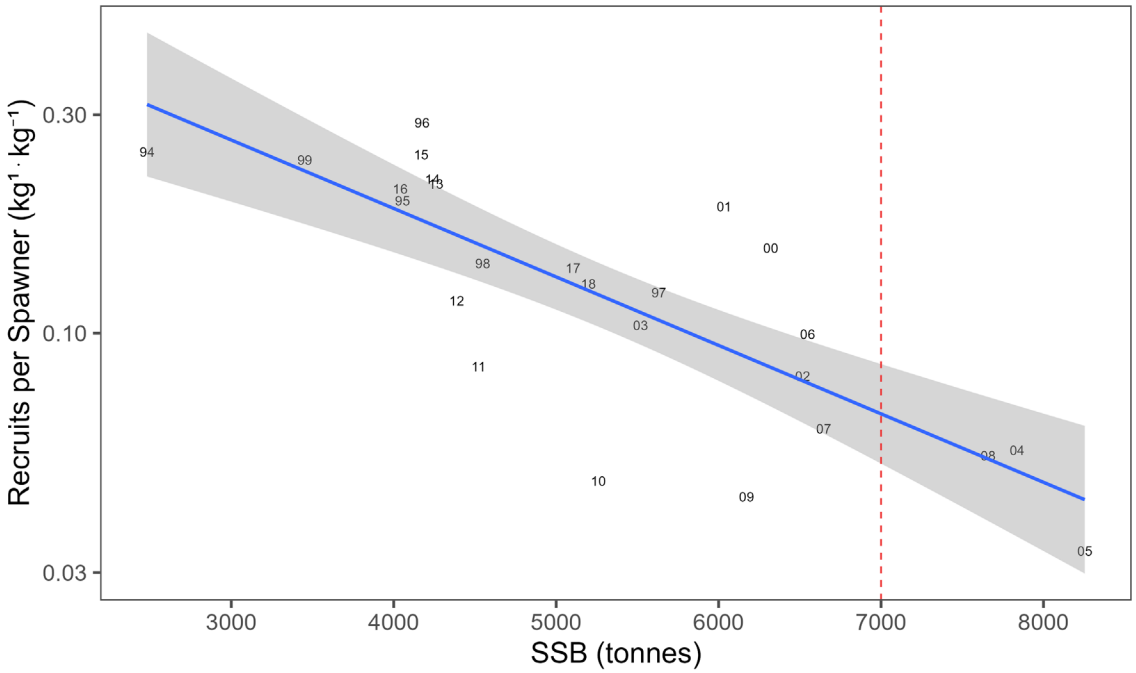

Figure 1. Relationship between recruits per spawner and spawning stock biomass (SSB; tonnes) in SFA 25A. The Ricker model is represented by the blue line with shaded 95% confidence interval. The vertical red dashed line represents the value used for the breakpoint analysis. The numbered points represent the year class of the recruits.

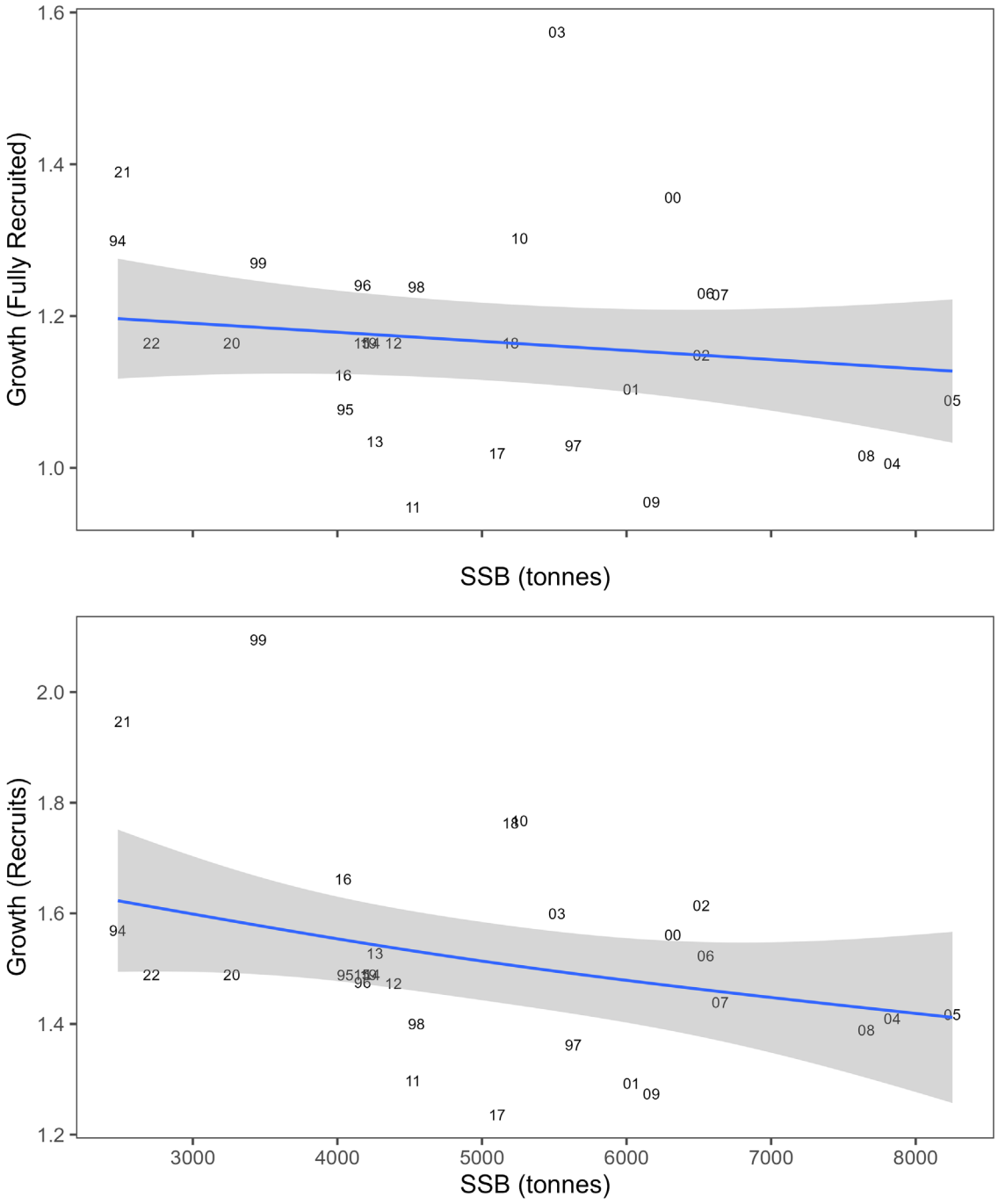

Figure 2. Relationship between fully recruited growth (top panel) and spawning stock biomass (SSB; tonnes) and recruit growth (bottom panel) and SSB (tonnes) in SFA 25A. The fit of the linear model is represented by the blue line with shaded 95% confidence interval. The numbered points represent the year.

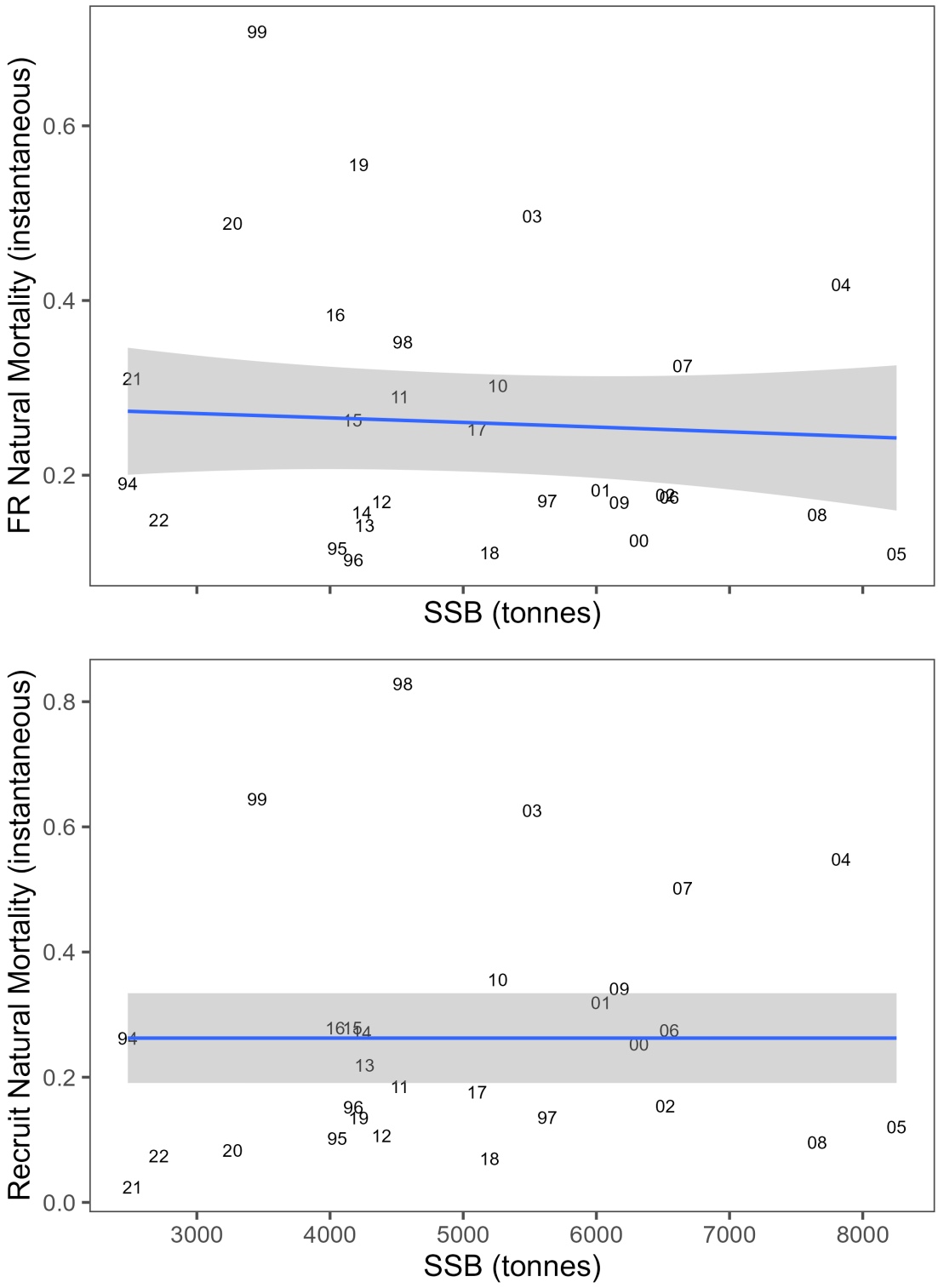

Figure 3. Relationship between fully-recruited (FR) natural mortality (top panel) and spawning stock biomass (SSB; tonnes) and recruit natural mortality (bottom panel) and SSB (tonnes) in SFA 25A. The fit of the linear model is represented by the blue line with shaded 95% confidence interval. The numbered points represent the year.

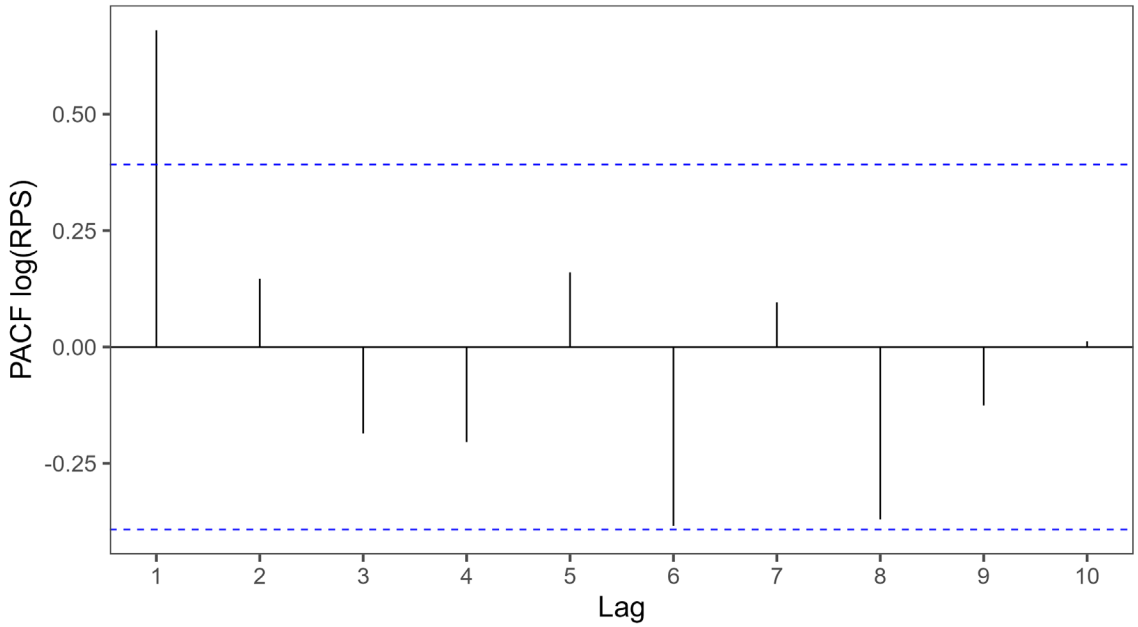

Figure 4. Autocorrelation (PCAF) for recruit per spawner (RPS) in SFA 25A. The vertical black lines represent the strength of the relationship at each lag, the horizontal blue lines represent the 95% significance level

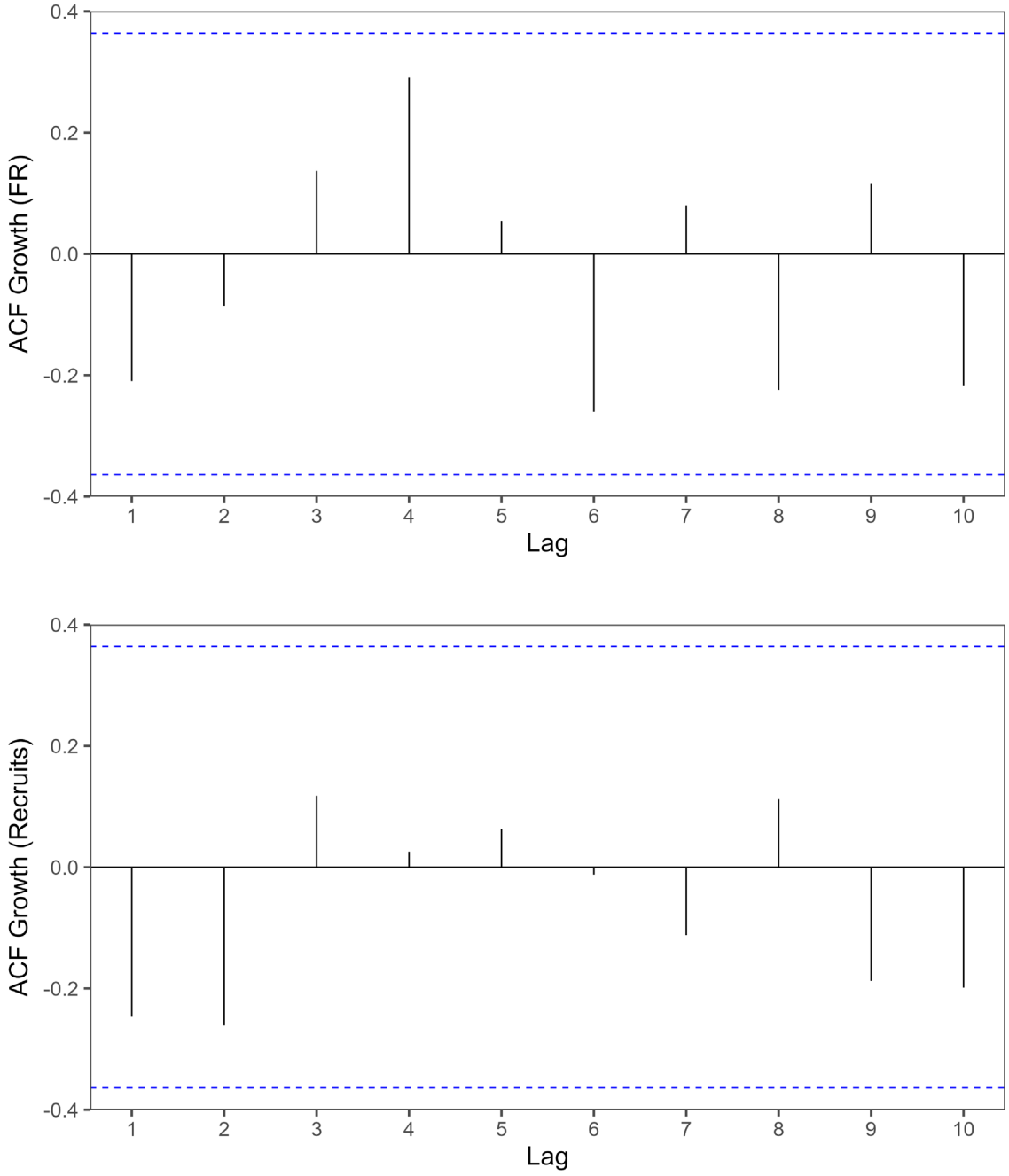

Figure 5. Autocorrelation (ACF) for fully recruited (FR) growth (top panel) and recruit growth (bottom panel) in SFA 25A. The vertical black lines represent the strength of the relationship at each lag, the horizontal blue lines represent the 95% significance level

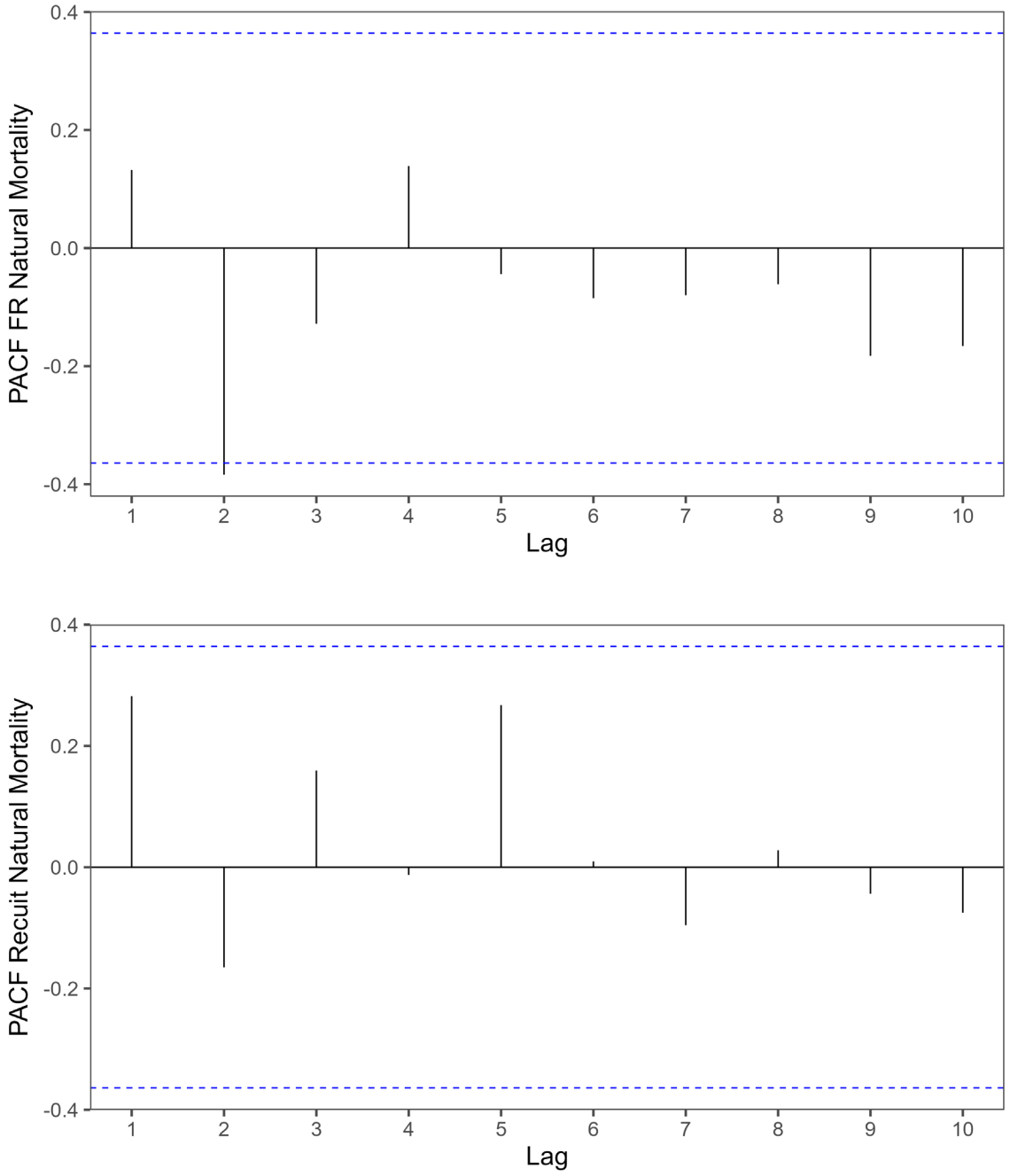

Figure 6. Autocorrelation (PCAF) for fully-recruited (FR) natural mortality (top panel) and recruit mortality (bottom panel) in SFA 25A. The vertical black lines represent the strength of the relationship at each lag, the horizontal blue lines represent the 95% significance level

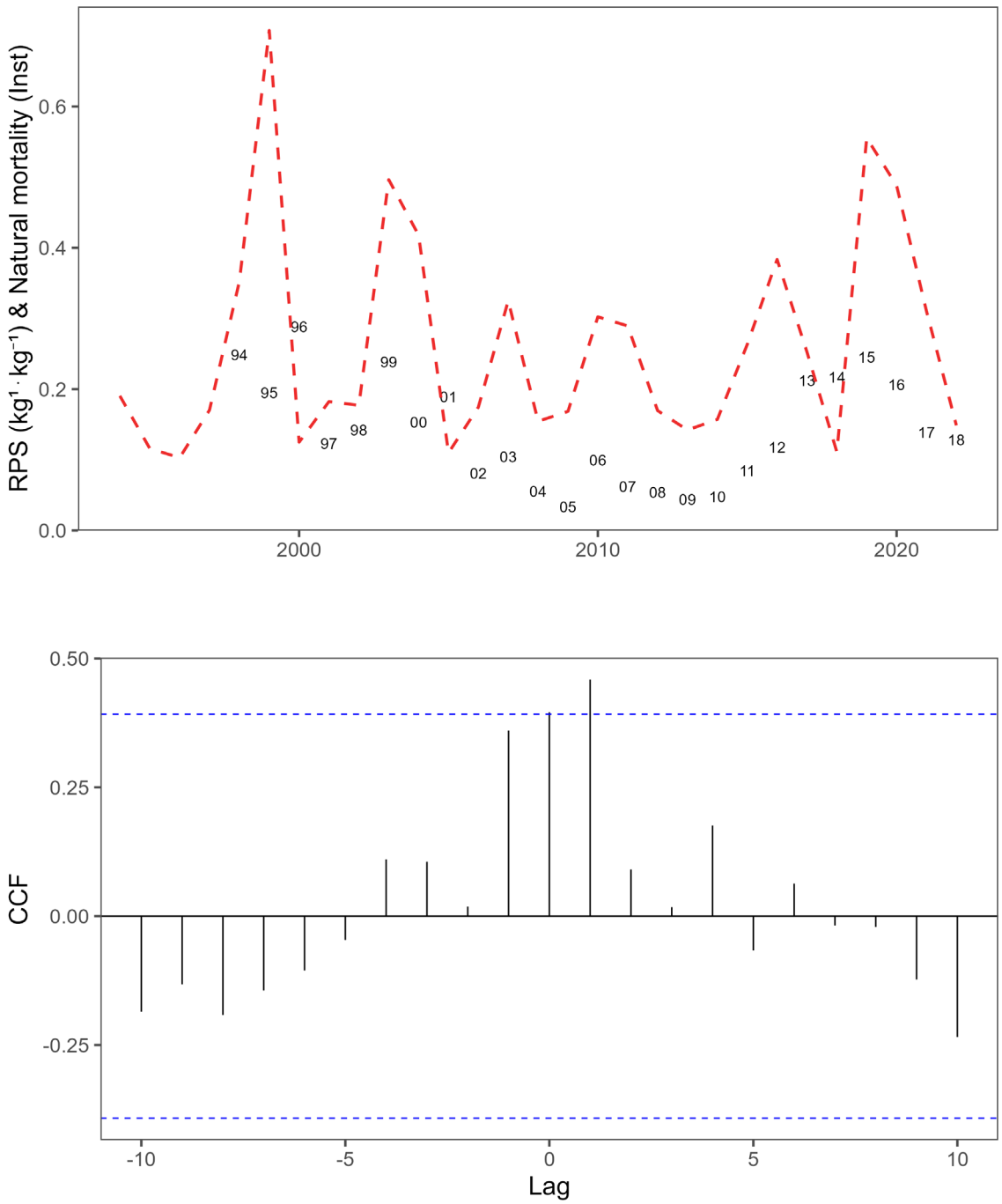

Figure 7. Relationship between fully-recruited natural mortality and recruit per spawner (RPS) in SFA 25A. The top panel is the time series of fully-recruited natural mortality (red dashed line) and RPS (text points represent the year class of the recruits). The bottom panel is the cross-correlation (CCF); here the vertical black lines represent the strength of the relationship at each lag, the horizontal blue lines represent the 95% significance level

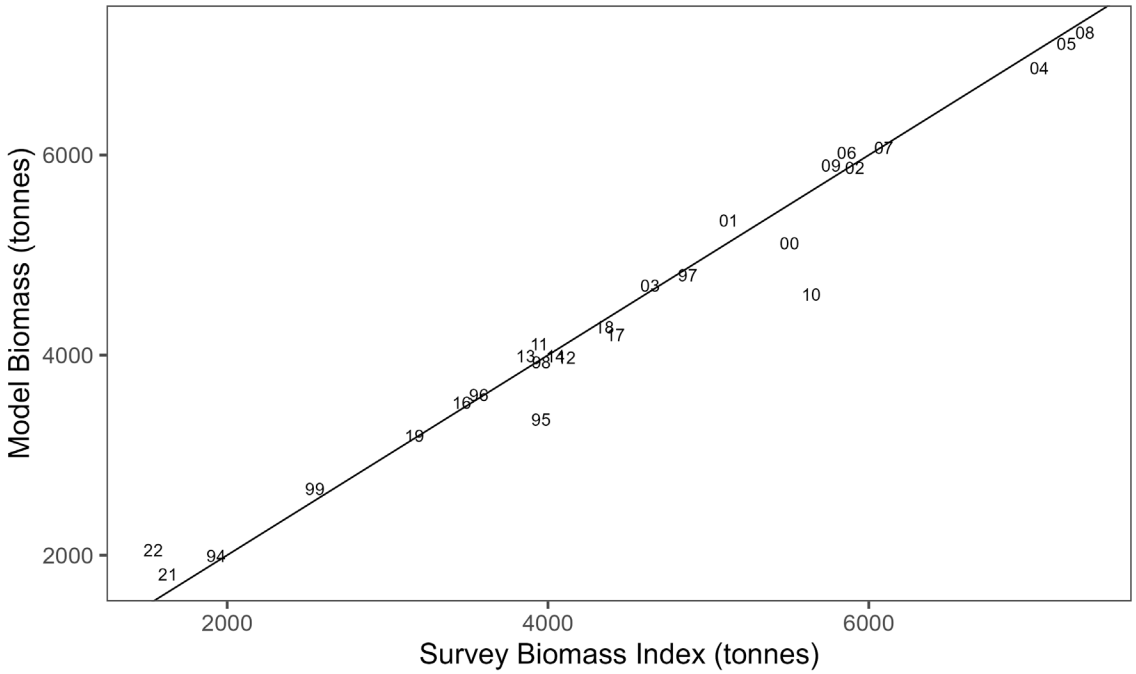

Figure 8. Relationship between the model biomass (tonnes) and the catchability corrected survey biomass index (tonnes) in SFA 25A. The text points represent the year and the black line is the 1:1 line (corrected for the median model catchability).

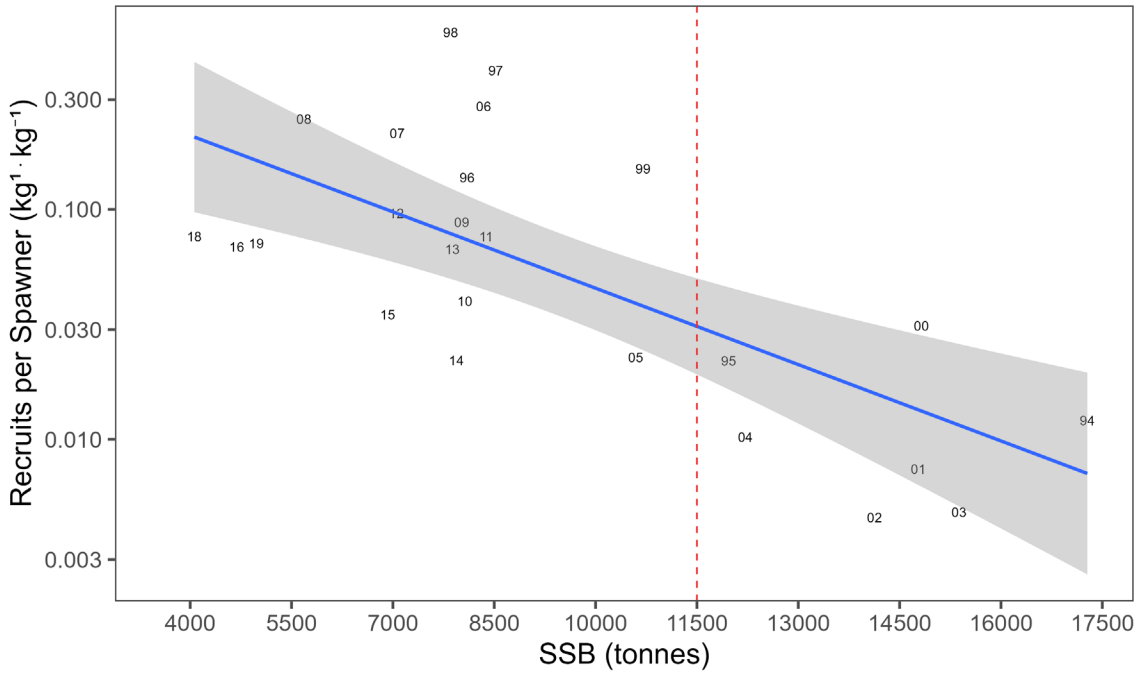

Figure 9. Relationship between recruits per spawner and spawning stock biomass (SSB; tonnes) in SFA 26A. The Ricker model is represented by the blue line with shaded 95% confidence interval. The vertical red dashed line represents the value used for the breakpoint analysis. The numbered points represent the year class of the recruits.

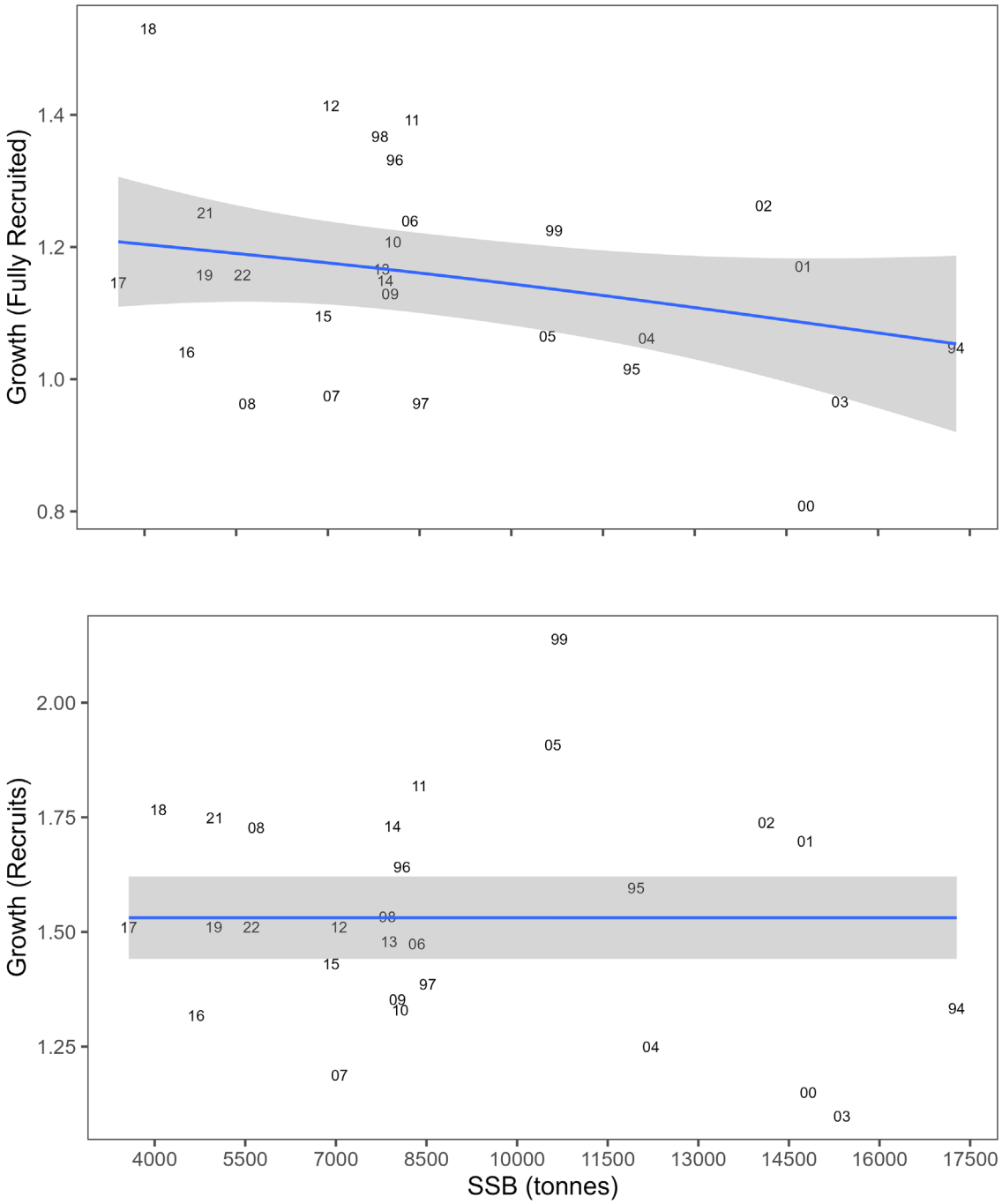

Figure 10. Relationship between fully recruited growth (top panel) and spawning stock biomass (SSB; tonnes) and recruit growth (bottom panel) and SSB (tonnes) in SFA 26A. The fit of the linear model is represented by the blue line with shaded 95% confidence interval. The numbered points represent the year.

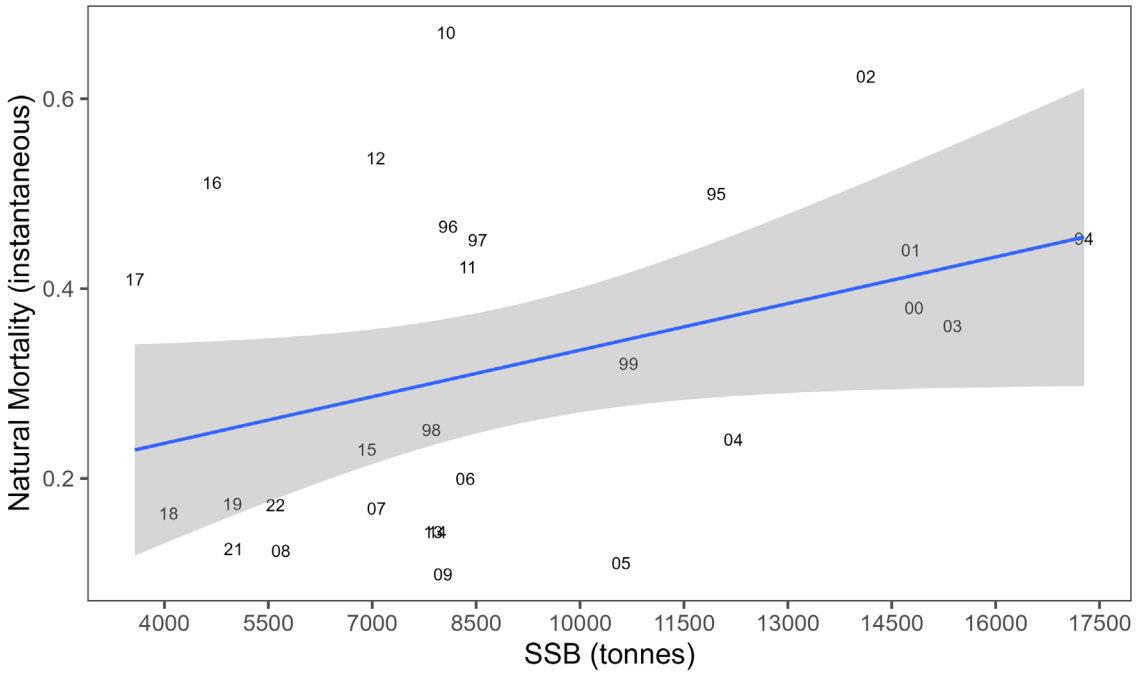

Figure 11. Relationship between natural mortality and spawning stock biomass (SSB; tonnes) in SFA 26A. The fit of the linear model is represented by the blue line with shaded 95% confidence interval. The numbered points represent the year.

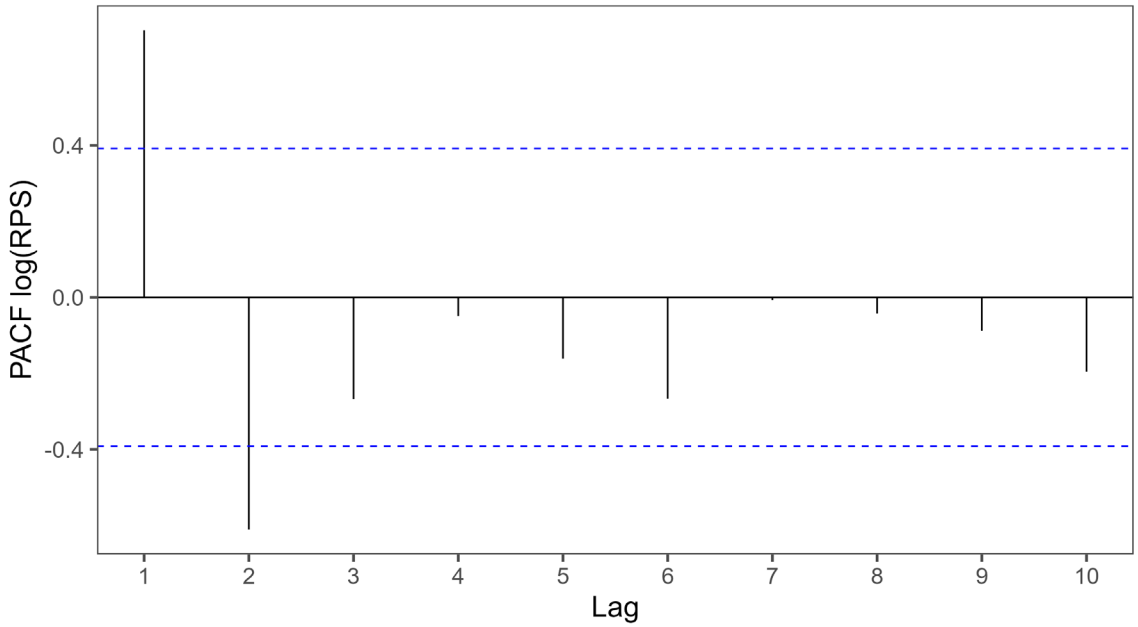

Figure 12. Autocorrelation (PCAF) for recruit per spawner (RPS) in SFA 26A. The vertical black lines represent the strength of the relationship at each lag, the horizontal blue lines represent the 95% significance level.

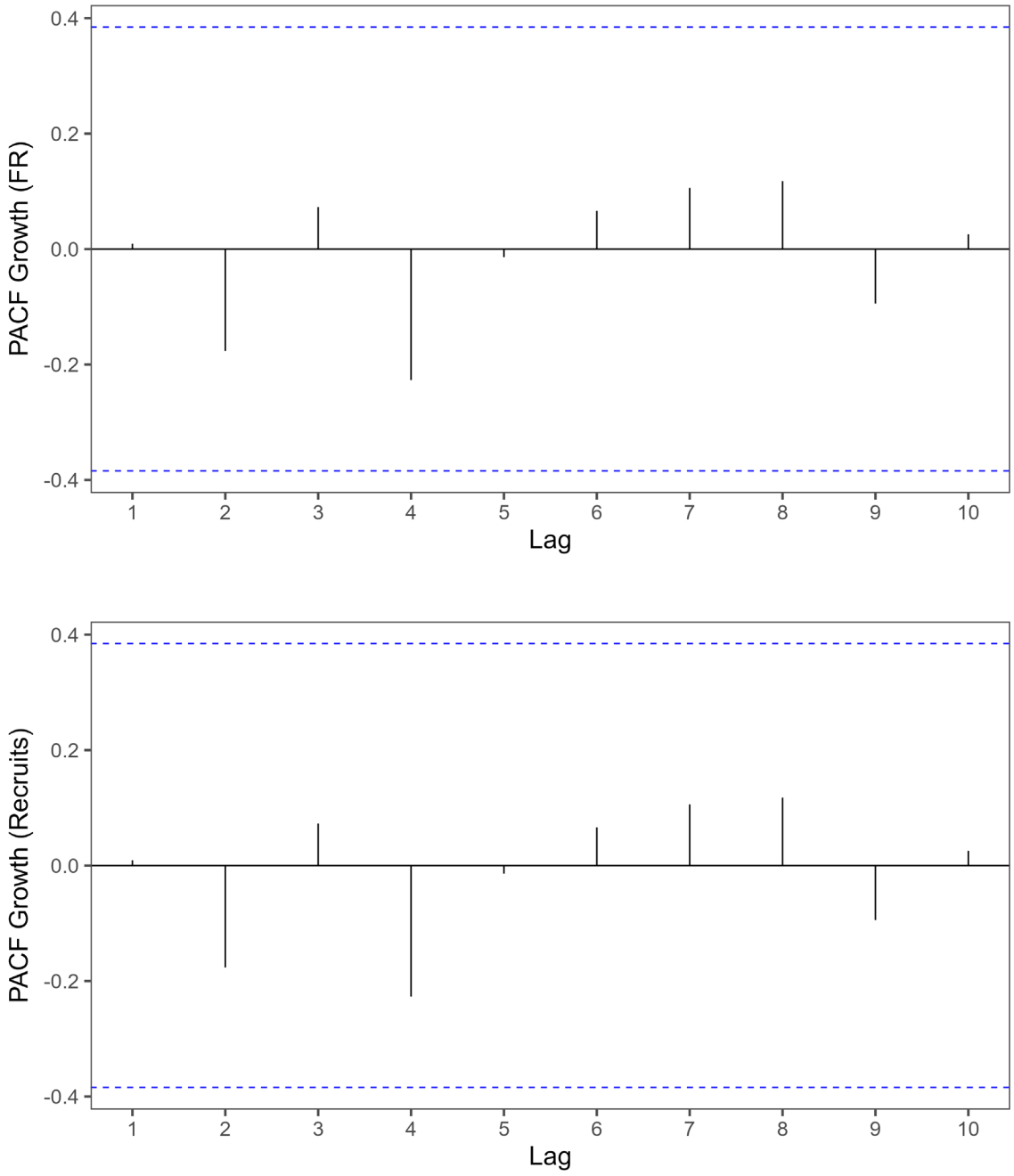

Figure 13. Autocorrelation (PCAF) for fully recruited growth (FR; top panel) and recruit growth (bottom panel) in SFA 26A. The vertical black lines represent the strength of the relationship at each lag, the horizontal blue lines represent the 95% significance level

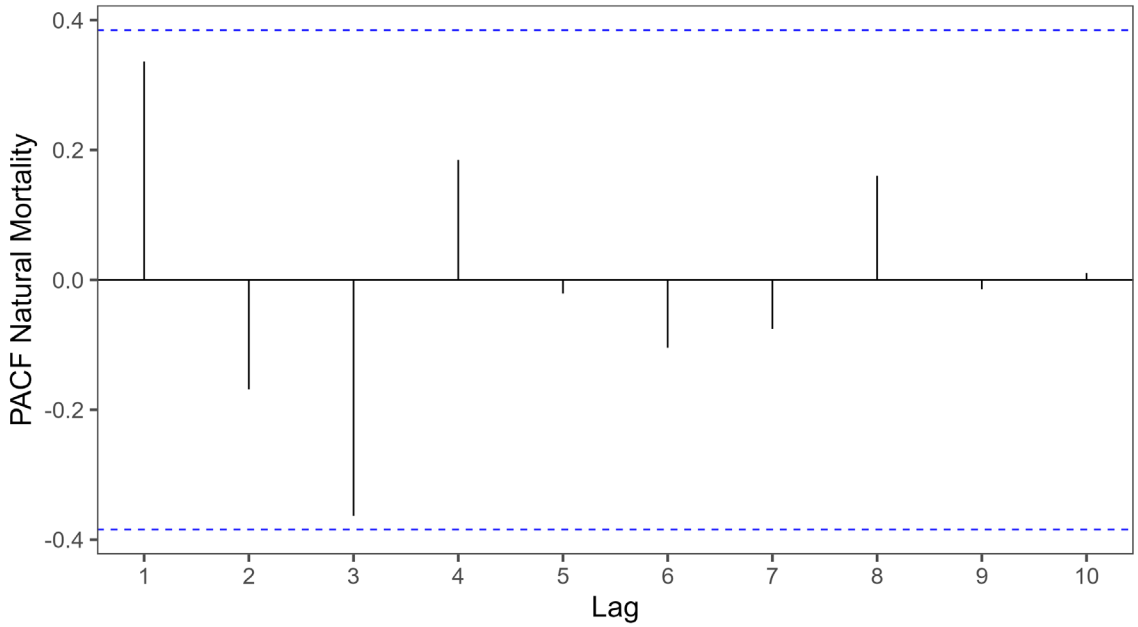

Figure 14. Autocorrelation (PCAF) for natural mortality in SFA 26A. The vertical black lines represent the strength of the relationship at each lag, the horizontal blue lines represent the 95% significance level

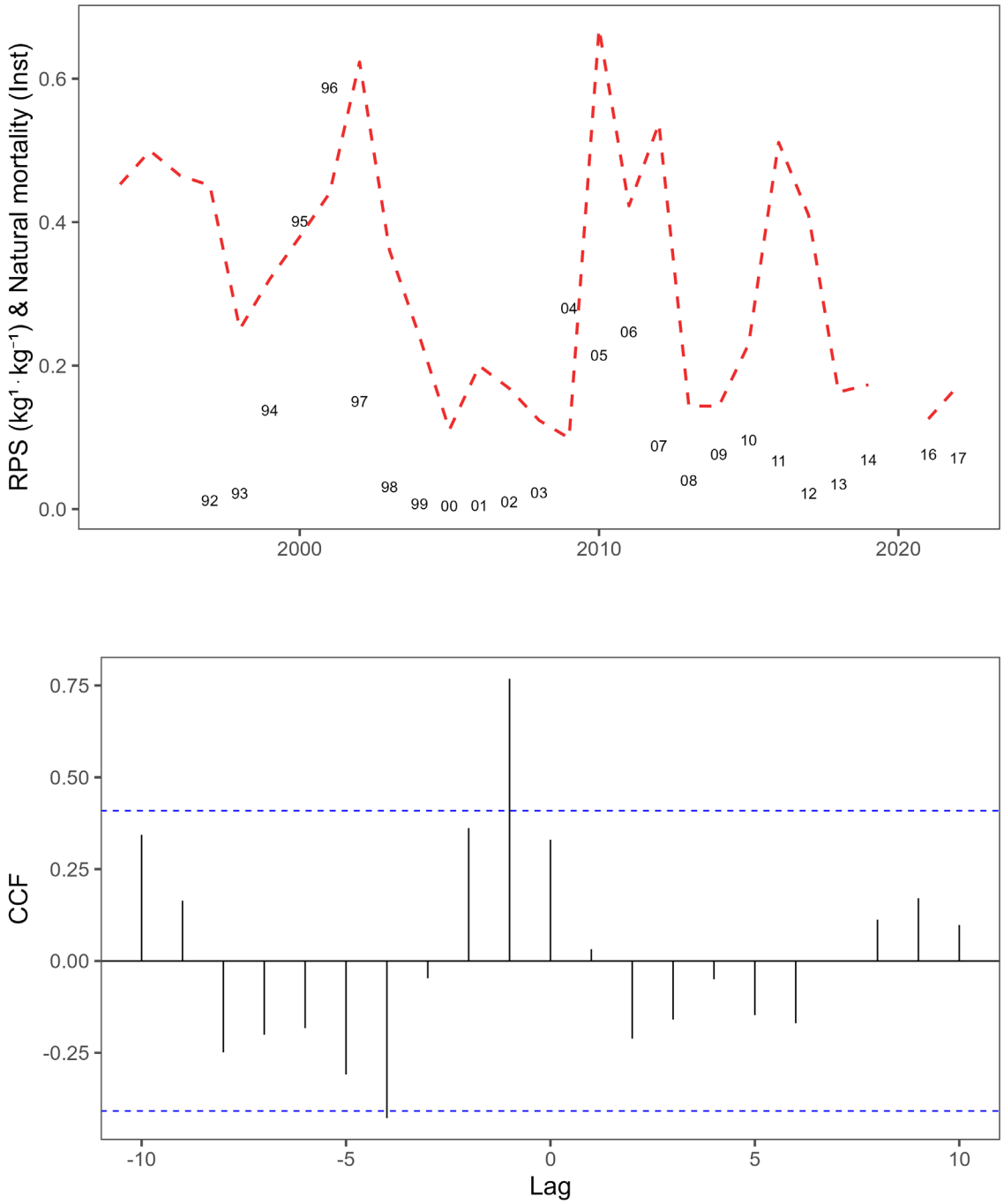

Figure 15. Relationship between fully-recruited natural mortality and recruit per spawner (RPS) in SFA 26A. The top panel is the time series of natural mortality (red dashed line) and RPS (text points represent the year class of the recruits). The bottom panel is the cross-correlation (CCF); here the vertical black lines represent the strength of the relationship at each lag, the horizontal blue lines represent the 95% significance level.

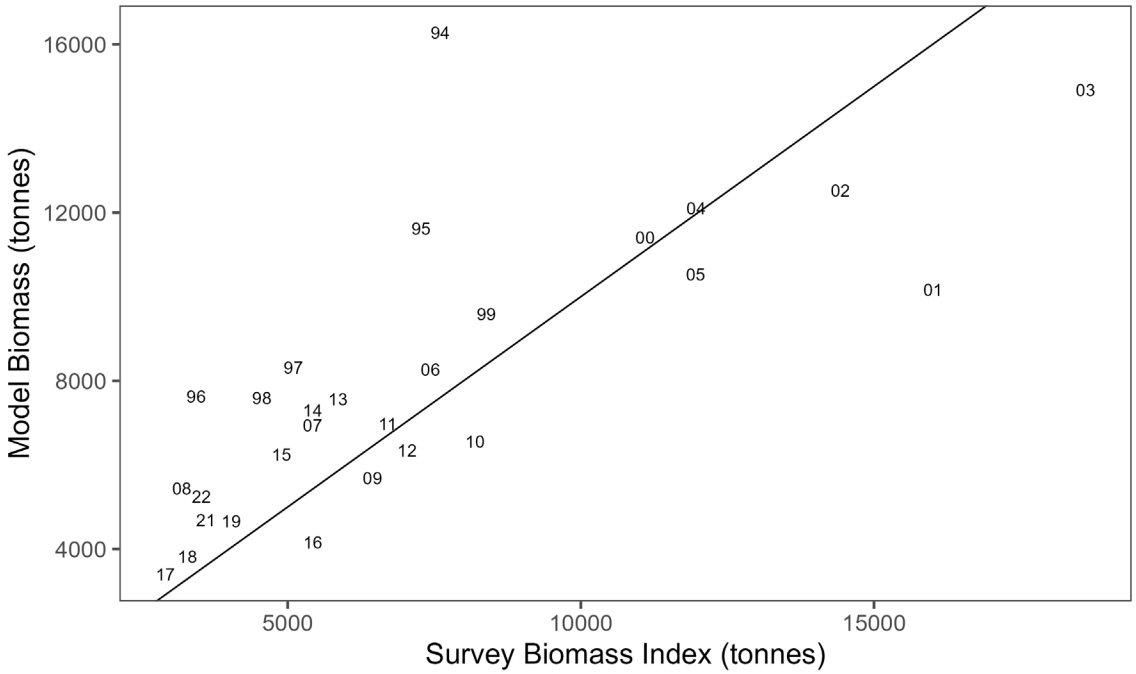

Figure 16. Relationship between the model biomass (tonnes) and the catchability corrected survey biomass index (tonnes) in SFA 26A. The text points represent the year and the black line is the 1:1 line (corrected for the median model catchability).

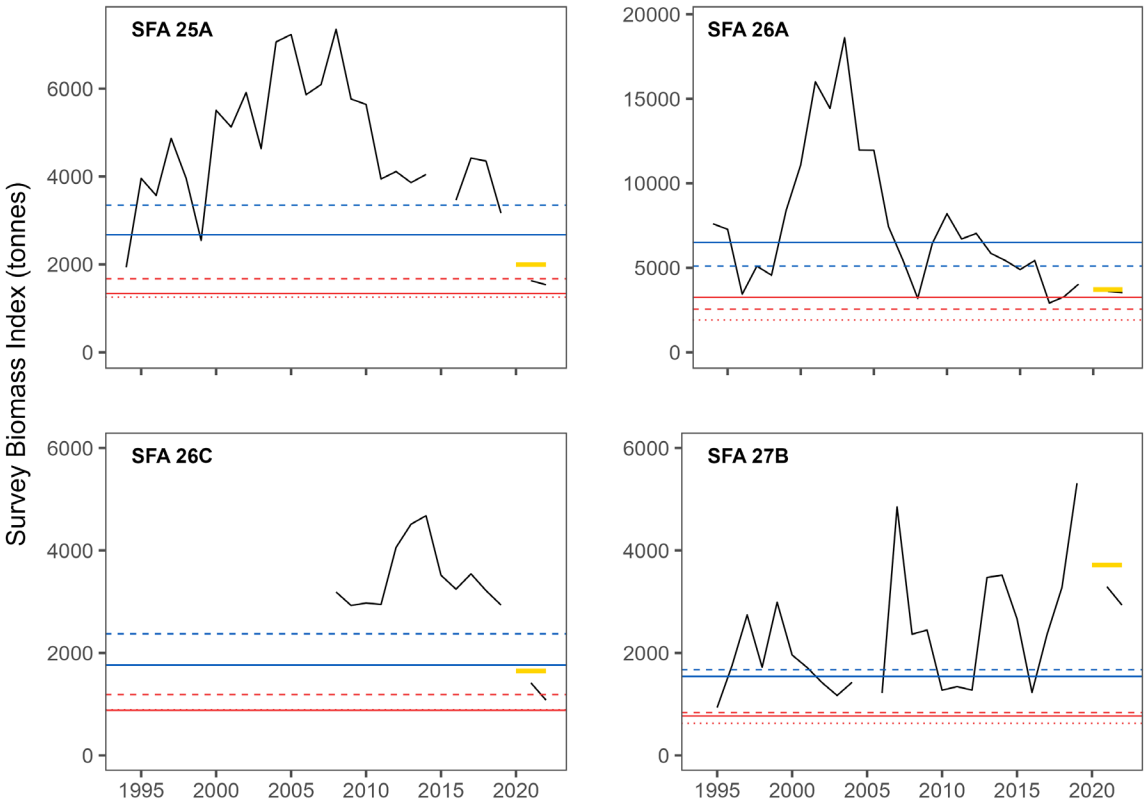

Figure 17. Catchability corrected survey biomass index time series (black line) for each of the areas. The geometric mean for the most recent three-years of data is represented by the thick yellow line. The limit reference points are represented by the red dotted line ($B_{MSY(30)}$), the dashed red line ($B_{MSY(40)}$), and the solid red line ($B_{0(20)}$). The upper stock references are represented by the dashed blue line ($B_{MSY(80)}$) and the solid blue line ($B_{0(40)}$).

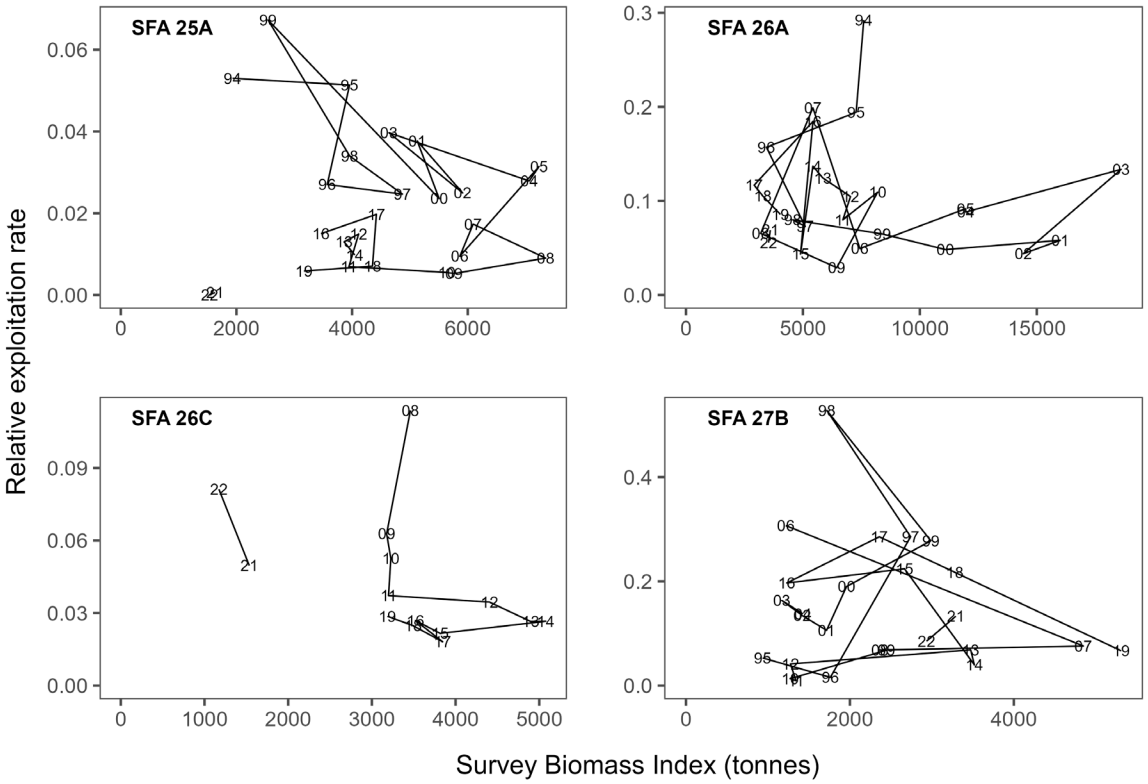

Figure 18. Phase plot for each of the areas. The relative exploitation rate is on the y-axis and catchability corrected survey biomass index is on the x-axis. The numbers on the plot represent the year.

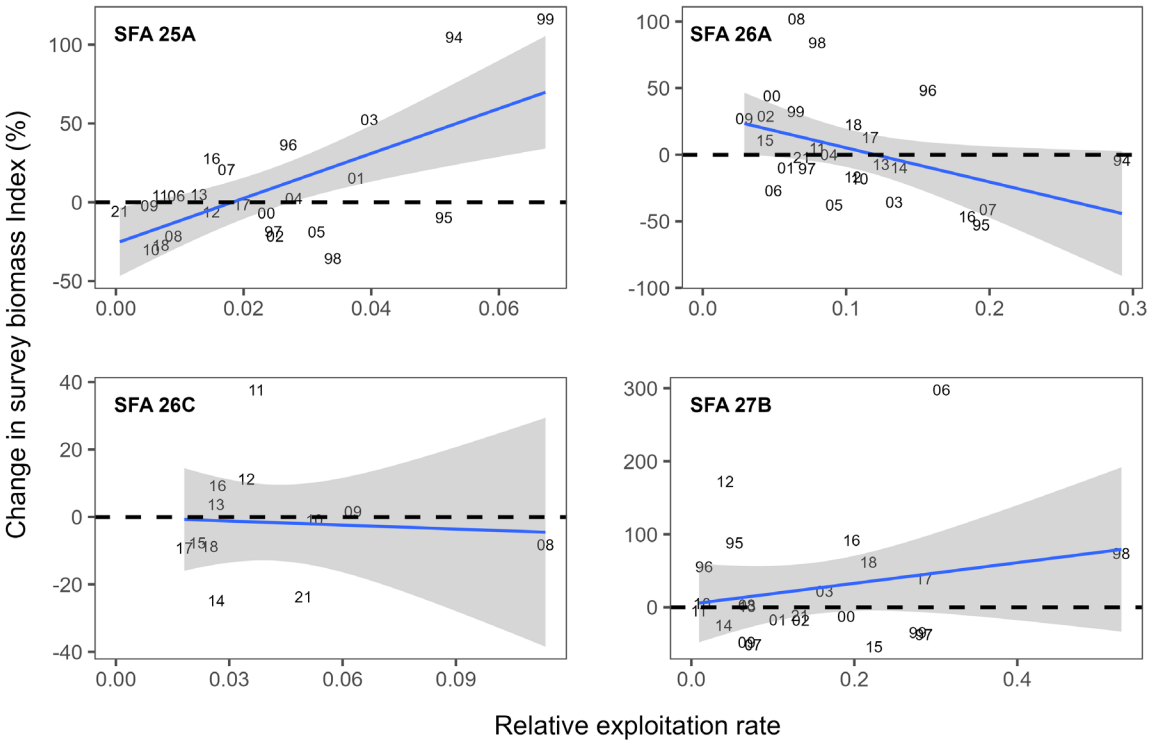

Figure 19. Percent change in the survey biomass index versus the relative exploitation rate for each area. The numbers on the plot represent the year (e.g., 14 is the change in biomass from 2014–2015 and the associated exploitation rate). The fit of the linear model is represented by the blue line with shaded 95% confidence interval.

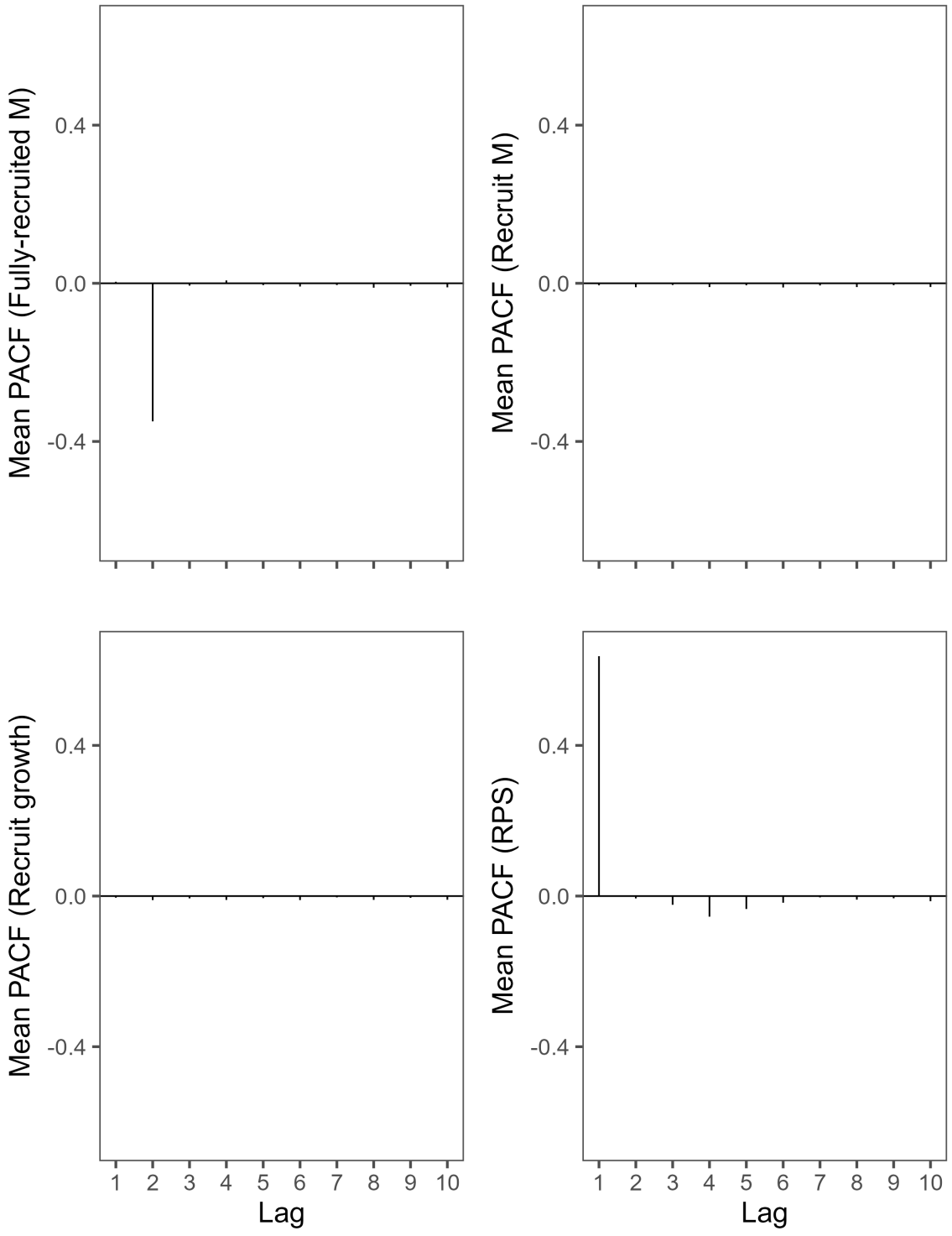

Figure 20. Mean estimate of the autocorrelation (PCAF) from the maximum sustainable yield simulation time series in SFA 25A using the B_{MSY} scenario. Shown are fully-recruited natural mortality (M; top left), recruit natural mortality (M; top right), recruit growth (bottom left), and recruit per spawner (RPS; bottom right). The vertical black lines represent the strength of the relationship at each lag.

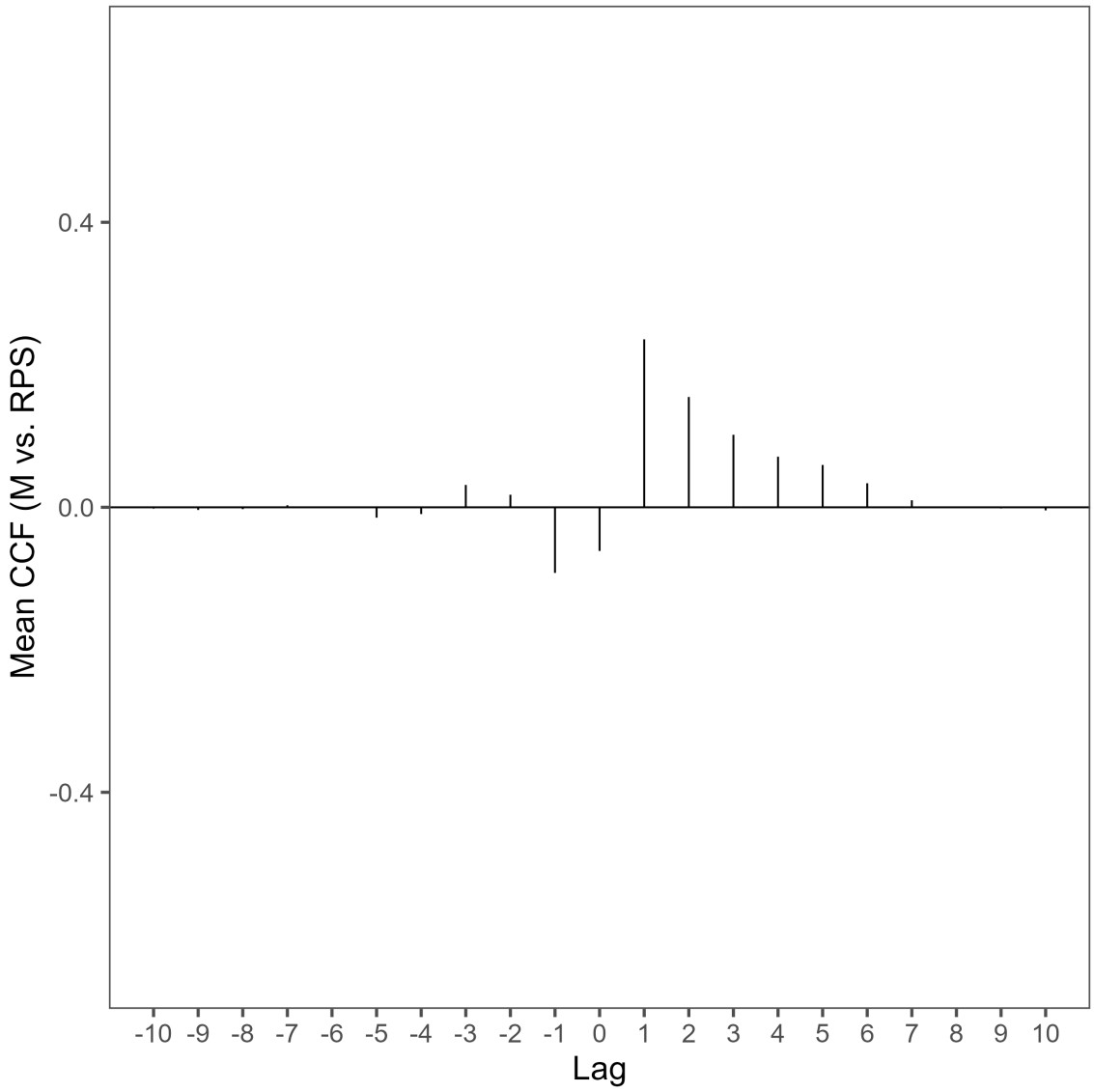

Figure 21. Mean estimate of the cross-correlation (CCF) of recruit per spawner (RPS) and fully-recruited natural mortality (M) from the maximum sustainable yield simulation time series in SFA 25A using the B_{MSY} scenario. The vertical black lines represent the strength of the relationship at each lag.

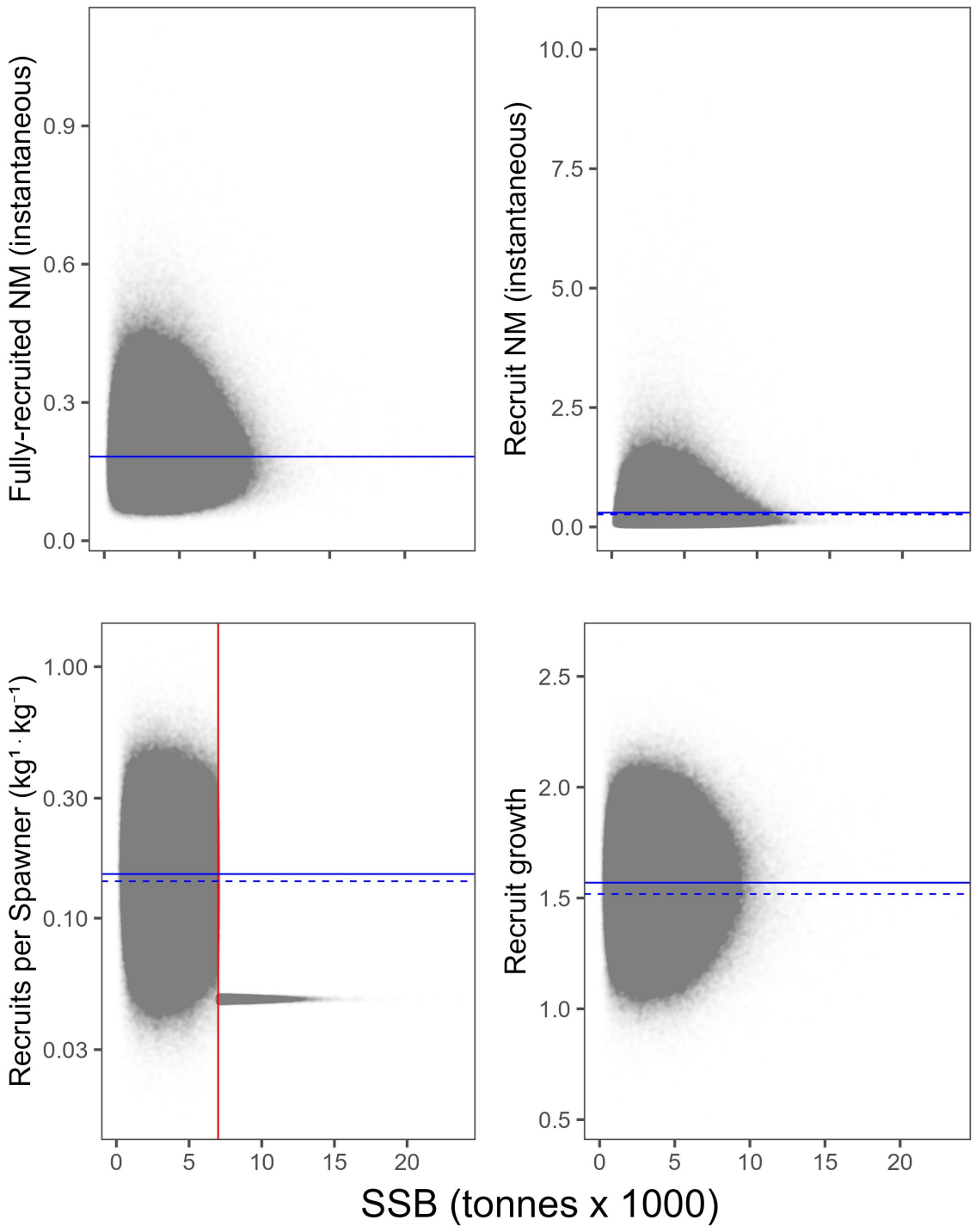

Figure 22. Relationship between the simulated parameter values and the simulated spawning stock biomass (SSB) estimates for SFA 25A using the maximum sustainable yield simulation B_{MSY} scenario. The blue solid horizontal line is the mean (median for the natural mortalities [NM]) value from the simulations, while the blue dashed line is the mean (median for the natural mortalities) estimated historical parameter estimate. The red vertical line on the lower left figure (recruit per spawner) represents the breakpoint.

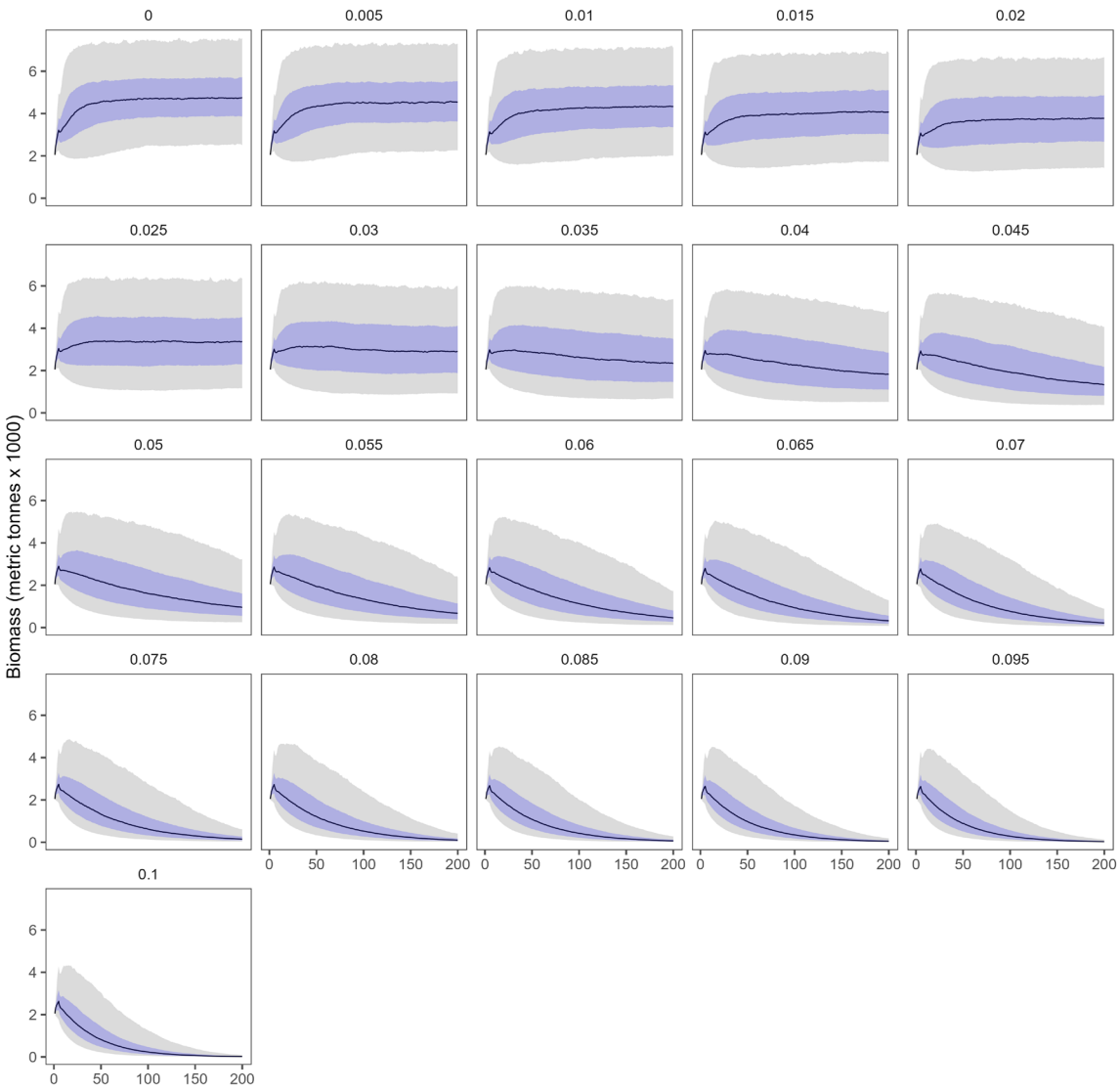

Figure 23. Median fully-recruited biomass estimates from the maximum sustainable yield simulations in SFA 25A, with 50% (blue) and 90% (grey) confidence intervals, for each exploitation rate scenario from the maximum sustainable yield simulations.

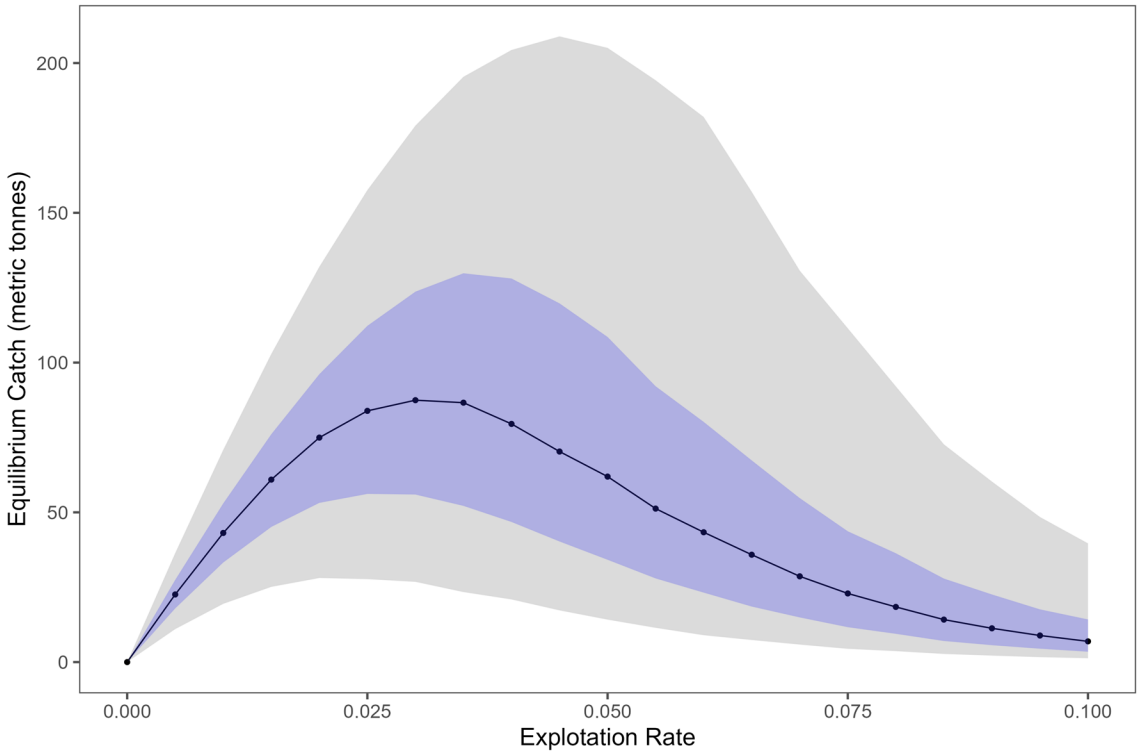

Figure 24. Median removals estimates in SFA 25A from the final 100 years of the maximum sustainable yield simulations, with 50% (blue) and 90% (grey) confidence intervals, for each exploitation rate scenario from the maximum sustainable yield simulations.

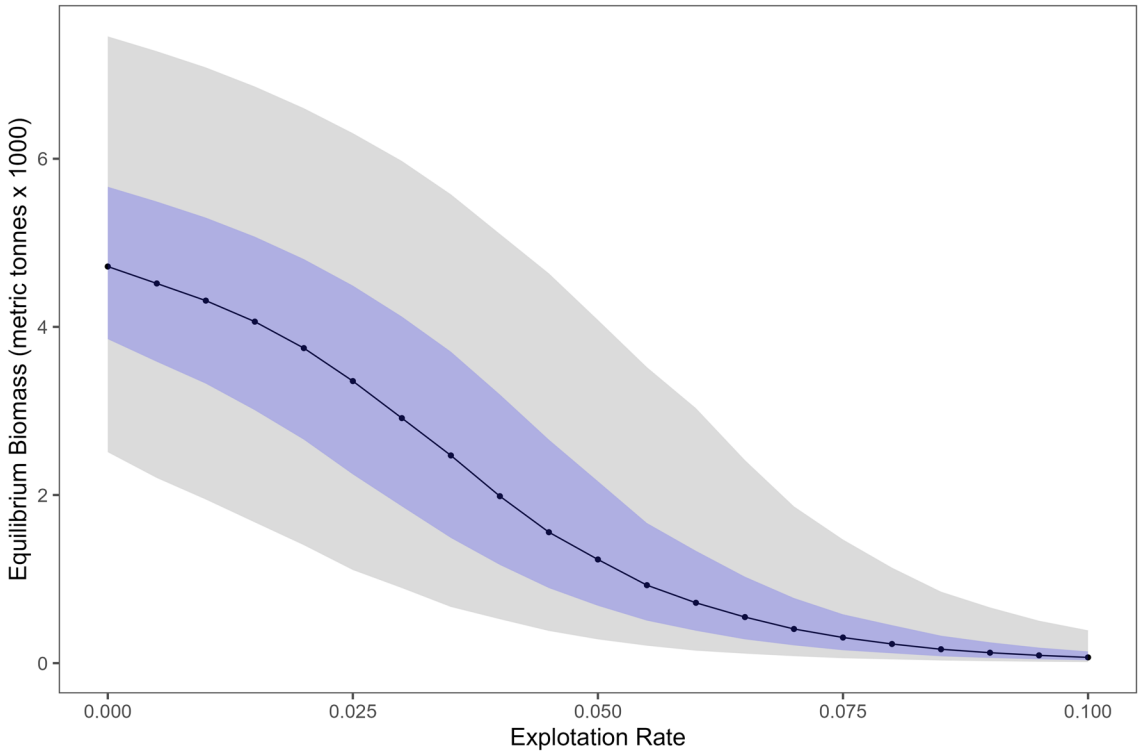

Figure 25. Median biomass estimates from the final 100 years of the simulations in SFA 25A, , with 50% (blue) and 90% (grey) confidence intervals, for each exploitation rate scenario from the maximum sustainable yield simulations.

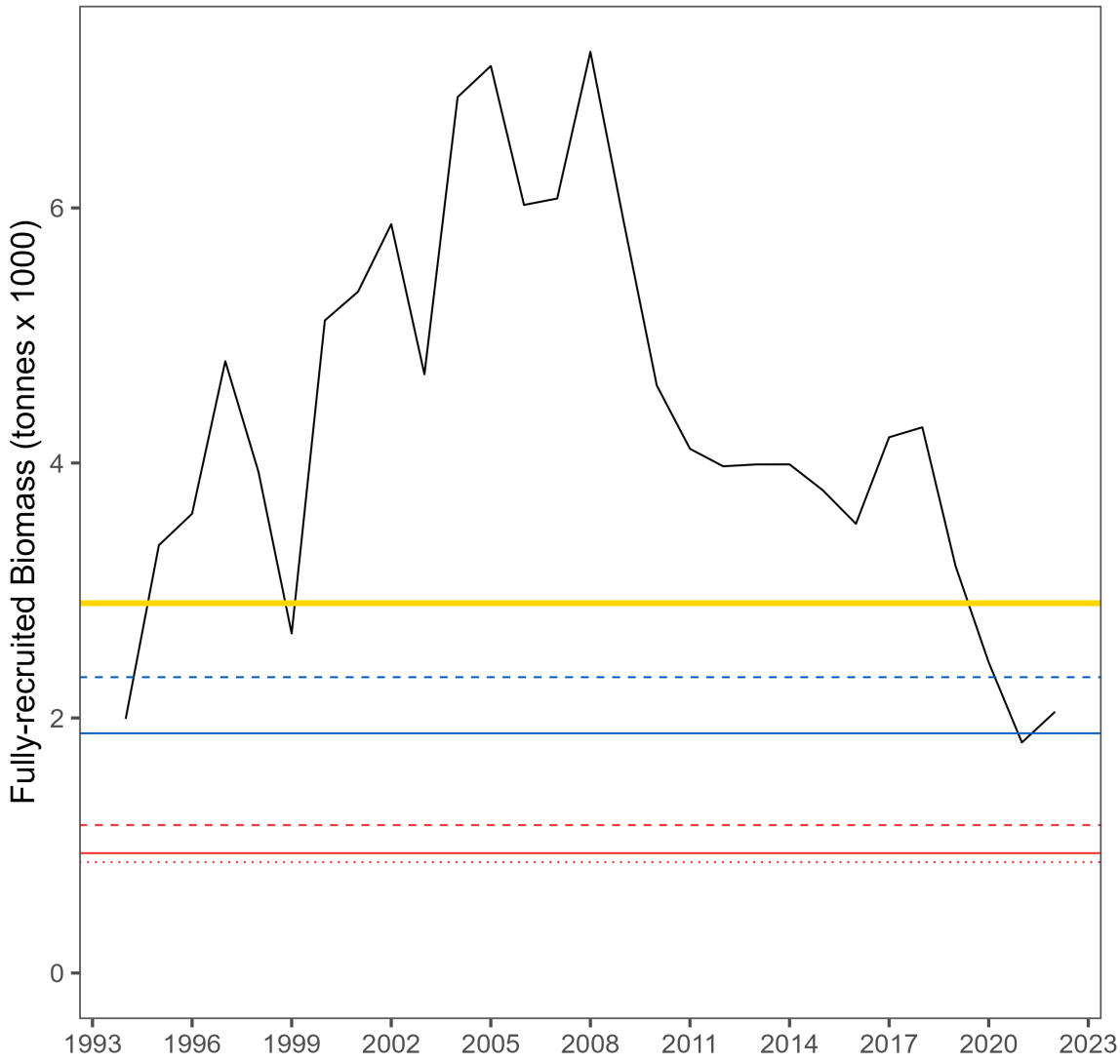

Figure 26. The historically modelled fully-recruited biomass time series (black line) relative to a suite of potential reference points in SFA 25A developed using the maximum sustainable yield simulations. The limit reference points are represented by the red dotted line ($B_{MSY(30)}$), the dashed red line ($B_{MSY(40)}$), and the solid red line ($B_{0(20)}$). The upper stock references are represented by the dashed blue line ($B_{MSY(80)}$) and the solid blue line ($B_{0(40)}$). The solid yellow line is the estimated biomass at maximum sustainable yield.

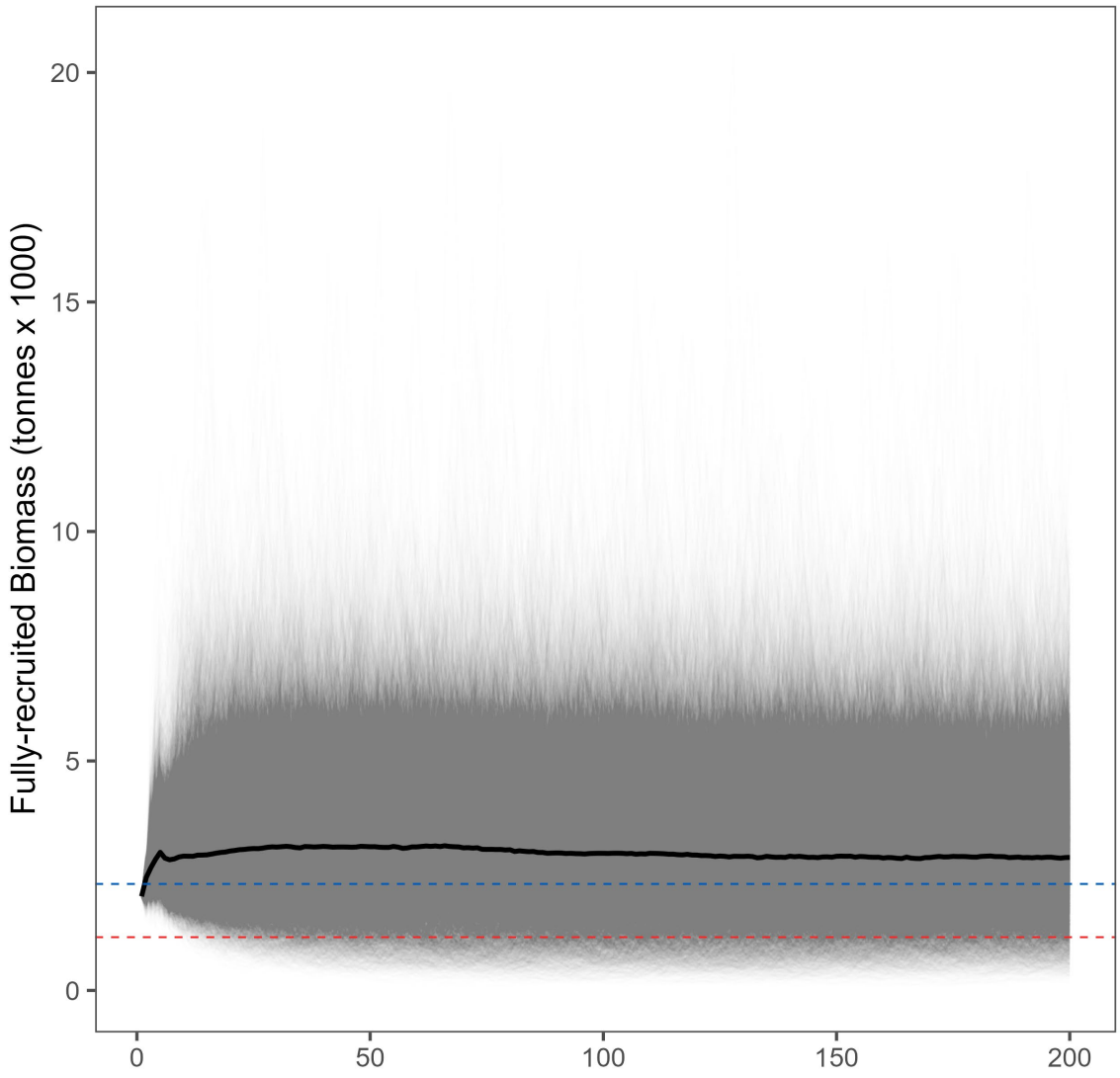

Figure 27. Maximum sustainable yield simulation time series projections of the fully-recruited biomass in SFA 25A when harvesting occurs at RR_{tar} (candidate target removal reference). A limit reference point ($B_{MSY(40)}$; dashed red line) and upper stock reference ($B_{MSY(80)}$; dashed blue line) are shown for reference. Each grey line represents one of the 10,000 realizations, and the thick black line is the median of the time series.

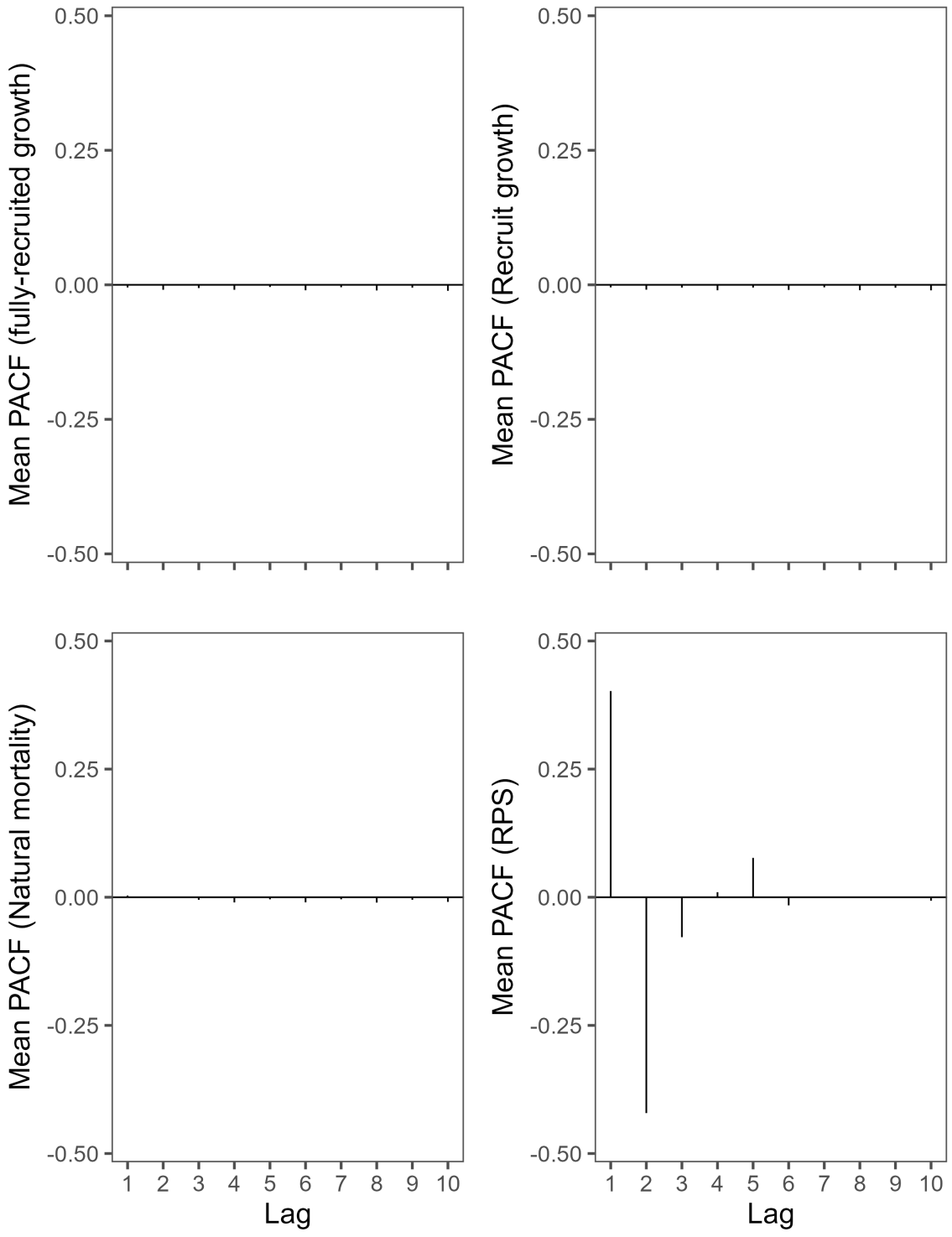

Figure 28. Mean estimate of the autocorrelation (PACF) from the maximum sustainable yield simulation time series in SFA 26A using the B_{MSY} simulation run. Shown are the fully-recruited growth (top left), recruit growth (top right), natural mortality (bottom left), and recruit per spanwer (RPS) (bottom right). The vertical black lines represent the strength of the relationship at each lag.

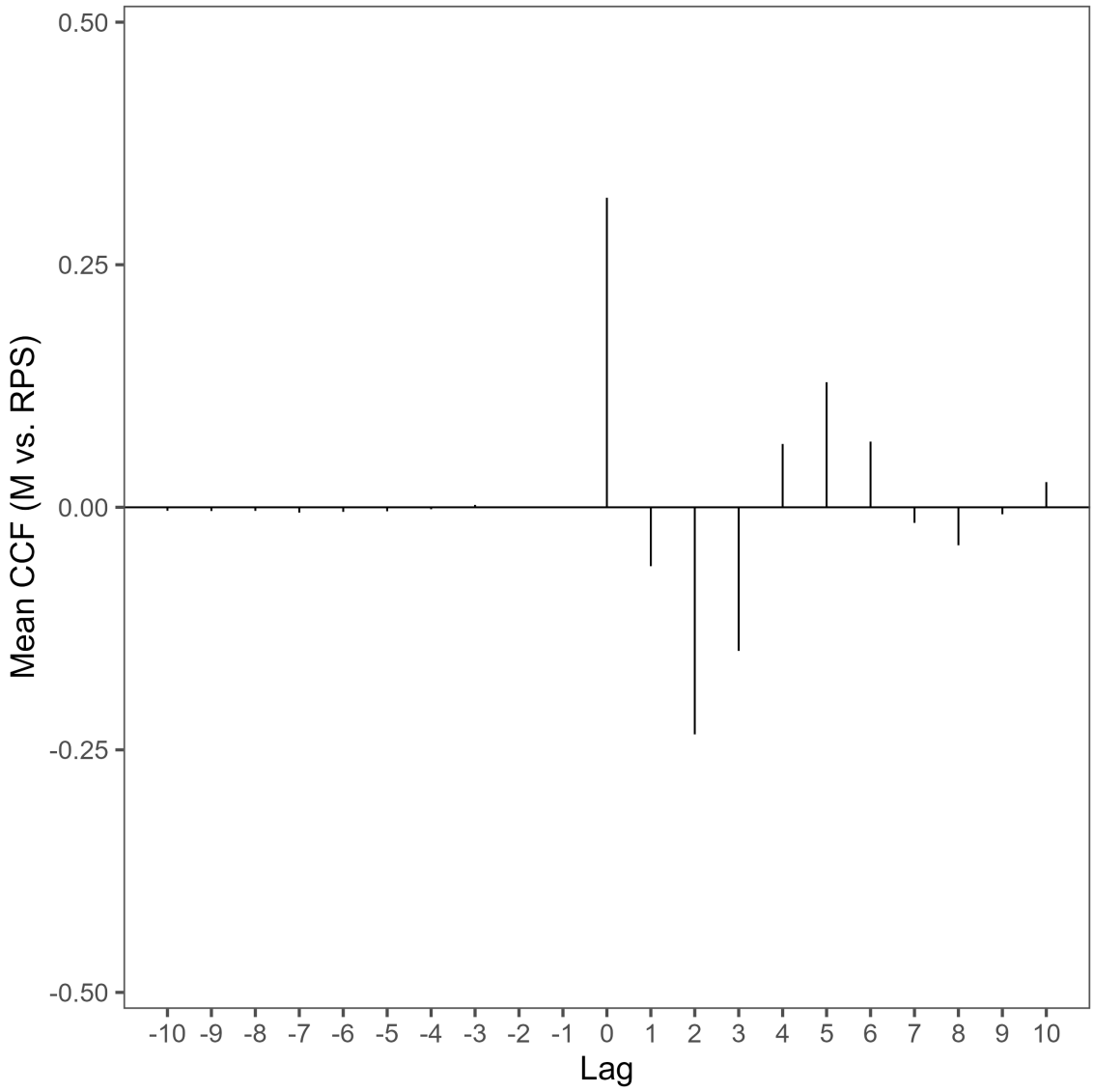

Figure 29. Mean estimate of the cross-correlation (CCF) of recruit per spawner (RPS) and fully-recruited natural mortality (M) from the maximum sustainable yield simulation time series in SFA 26A using the B_{MSY} simulation run. The vertical black lines represent the strength of the relationship at each lag.

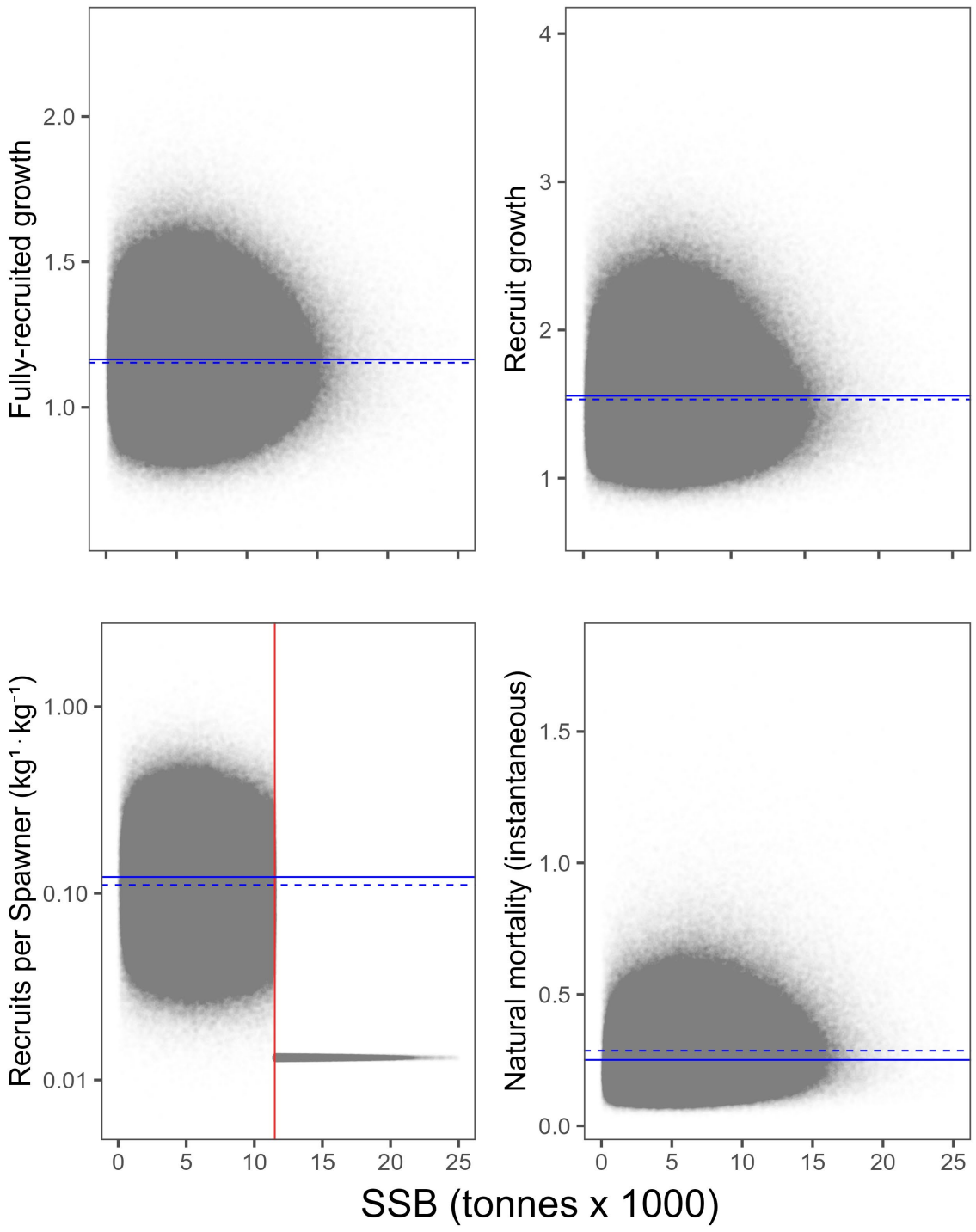

Figure 30. Relationship between the simulated parameter values and the simulated spawning stock biomass (SSB) estimates for SFA 26A using the B_{MSY} scenario from the maximum sustainable yield simulations. The blue solid horizontal line is the mean (median for natural mortality) value from the simulations, while the blue dashed line is the mean (median for natural mortality) estimated historical parameter estimate. The red vertical line on the lower left recruit per spawner figure represents the breakpoint.

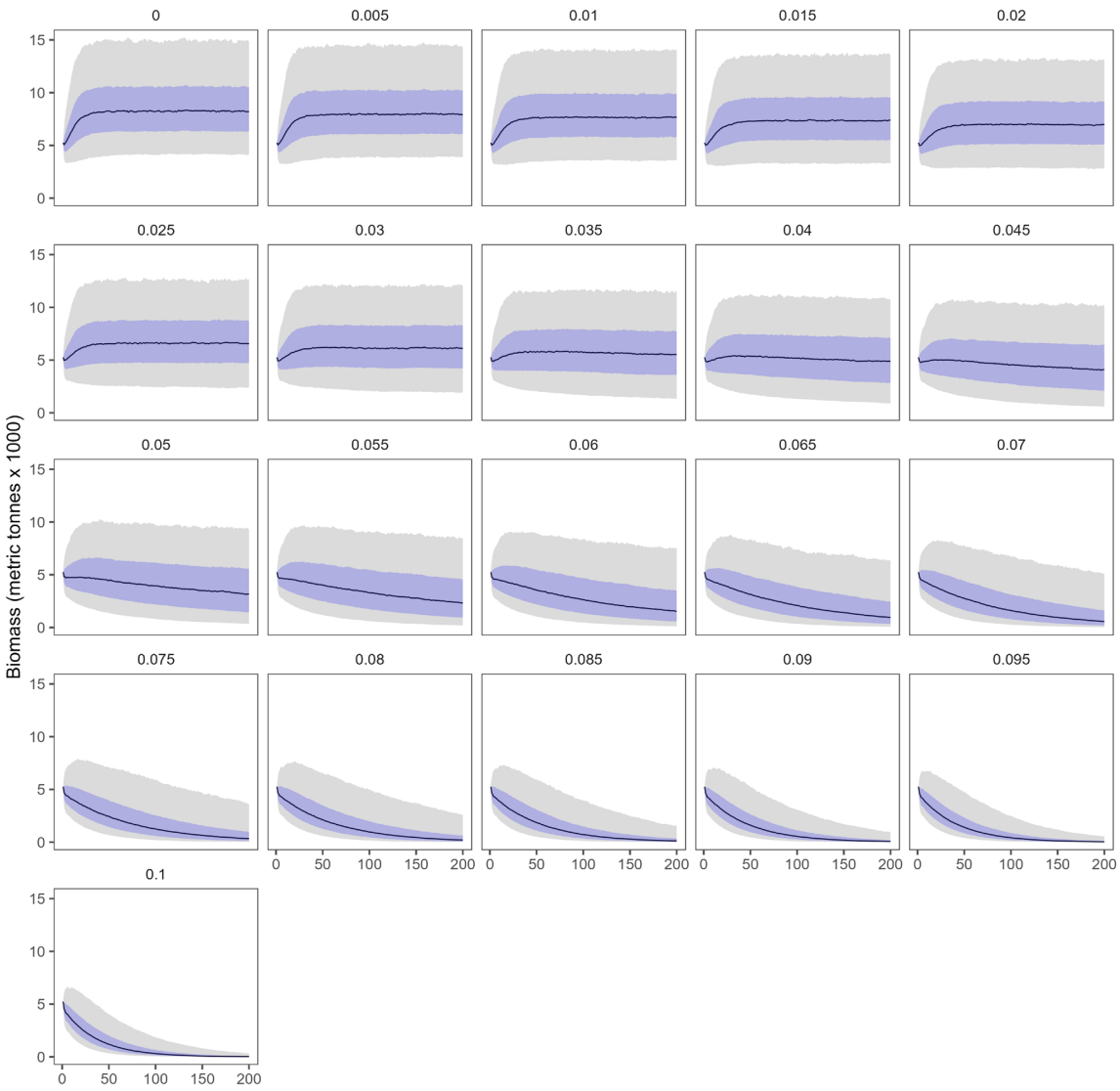

Figure 31. Median fully-recruited biomass estimates in SFA 26A for each exploitation rate scenario from the maximum sustainable yield simulations. The blue shading represents the 50% confidence interval and the grey shading is the 90% confidence interval.

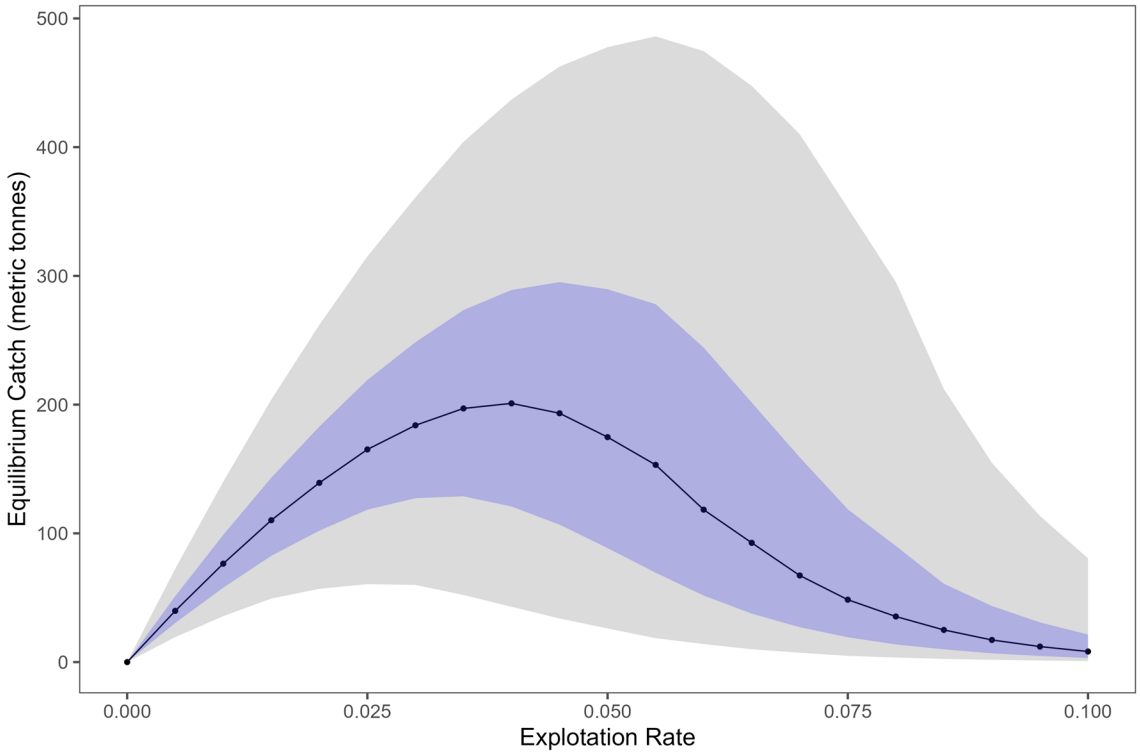

Figure 32. Median removals estimates in SFA 26A from the final 100 years for each exploitation rate scenario from the maximum sustainable yield simulations. The blue shading represents the 50% confidence interval and the grey shading is the 90% confidence interval.

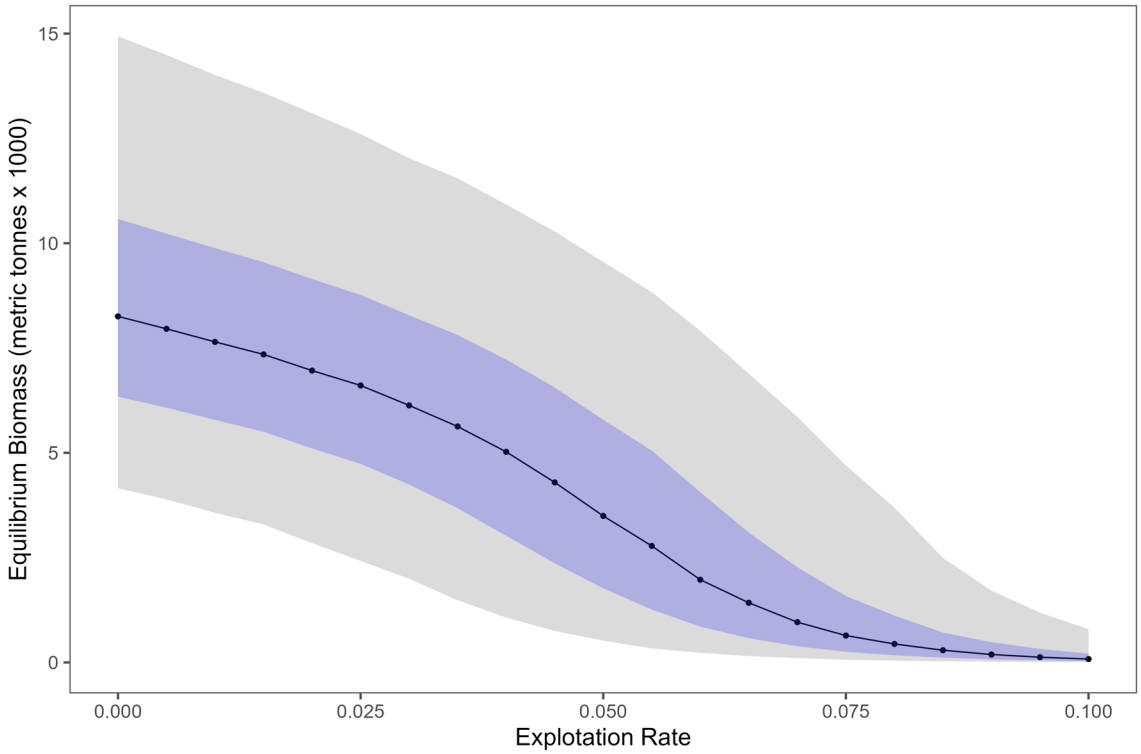

Figure 33. Median biomass estimates from the final 100 years for each exploitation rate scenario from the maximum sustainable yield simulations. The blue shading represents the 50% confidence interval and the grey shading is the 90% confidence interval.

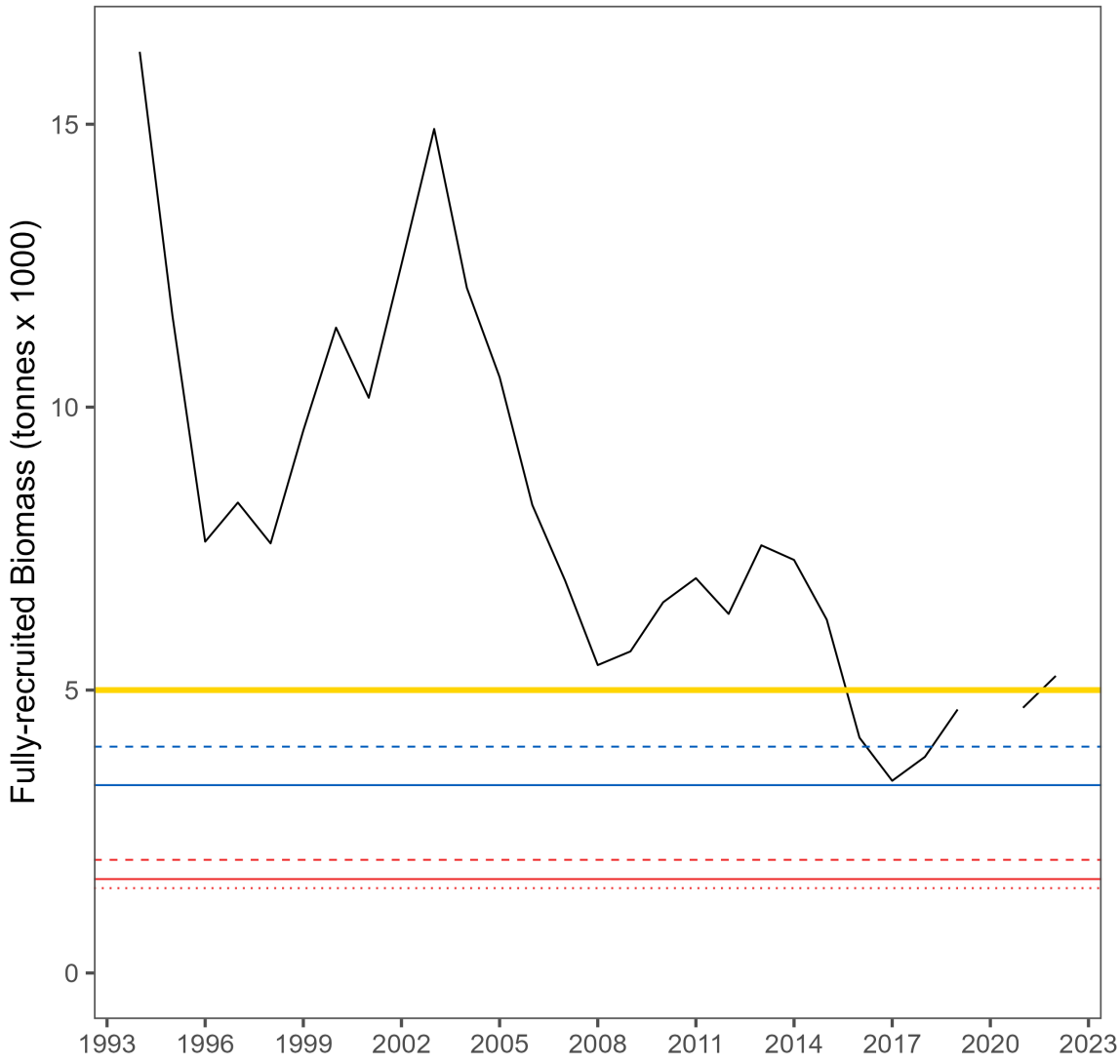

Figure 34. The historically modelled fully-recruited biomass time series (black line) relative to a suite of potential reference points in SFA 26A developed using the maximum sustainable yield simulations. The limit reference points are represented by the red dotted line ($B_{MSY(30)}$), the dashed red line ($B_{MSY(40)}$), and the solid red line ($B_{0(20)}$). The upper stock references are represented by the dashed blue line ($B_{MSY(80)}$) and the solid blue line ($B_{0(40)}$). The solid yellow line is the estimated biomass at maximum sustainable yield.

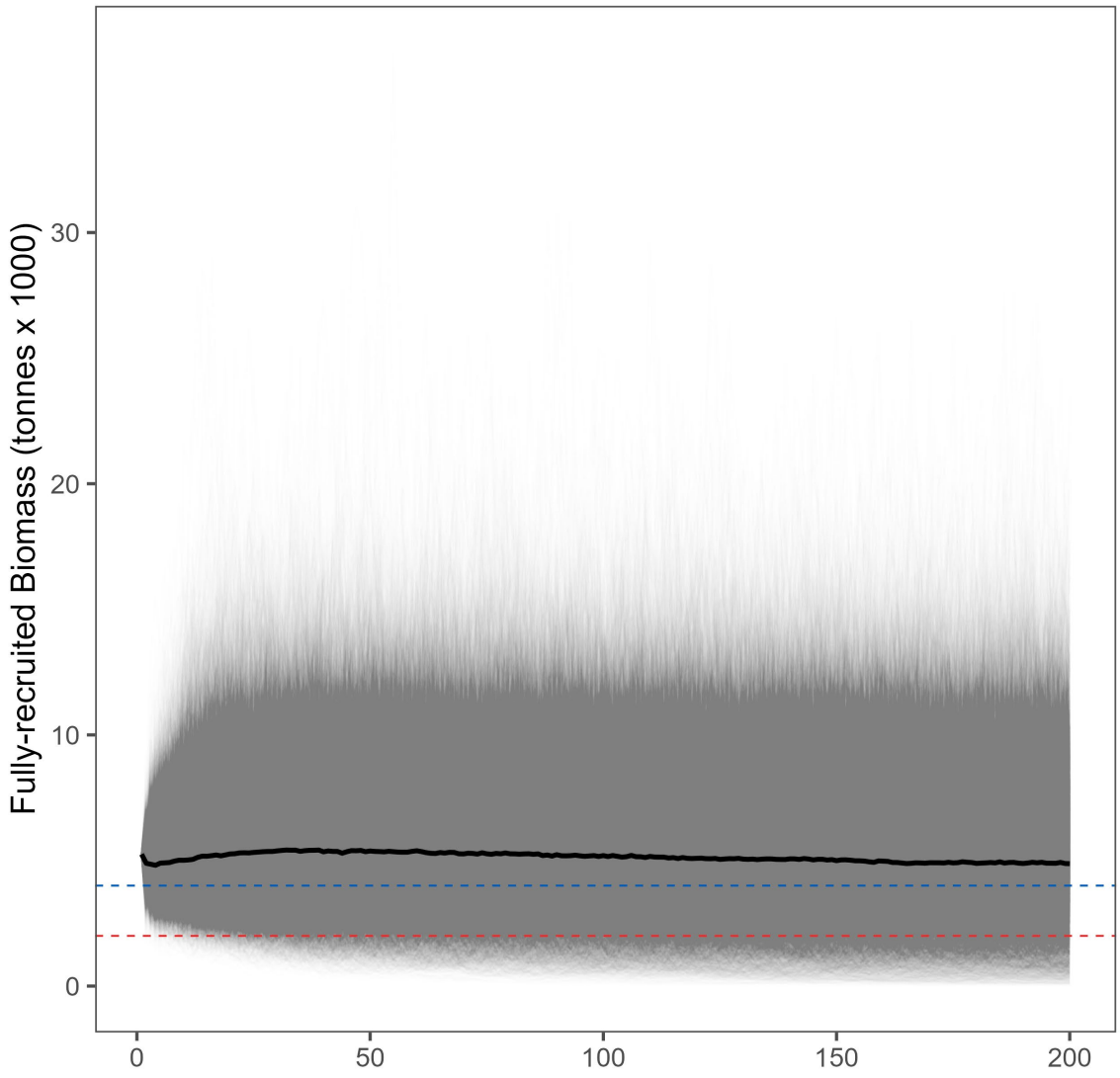

Figure 35. Maximum sustainable yield simulation time series of fully-recruited biomass projections in SFA 26A when harvesting occurs at RR_{tar} (candidate target removal reference). A limit reference point ($B_{MSY(40)}$; dashed red line) and upper stock reference ($B_{MSY(80)}$; dashed blue line) are shown for reference. Each grey line represents one of the 10,000 realizations, and the thick black line is the median.

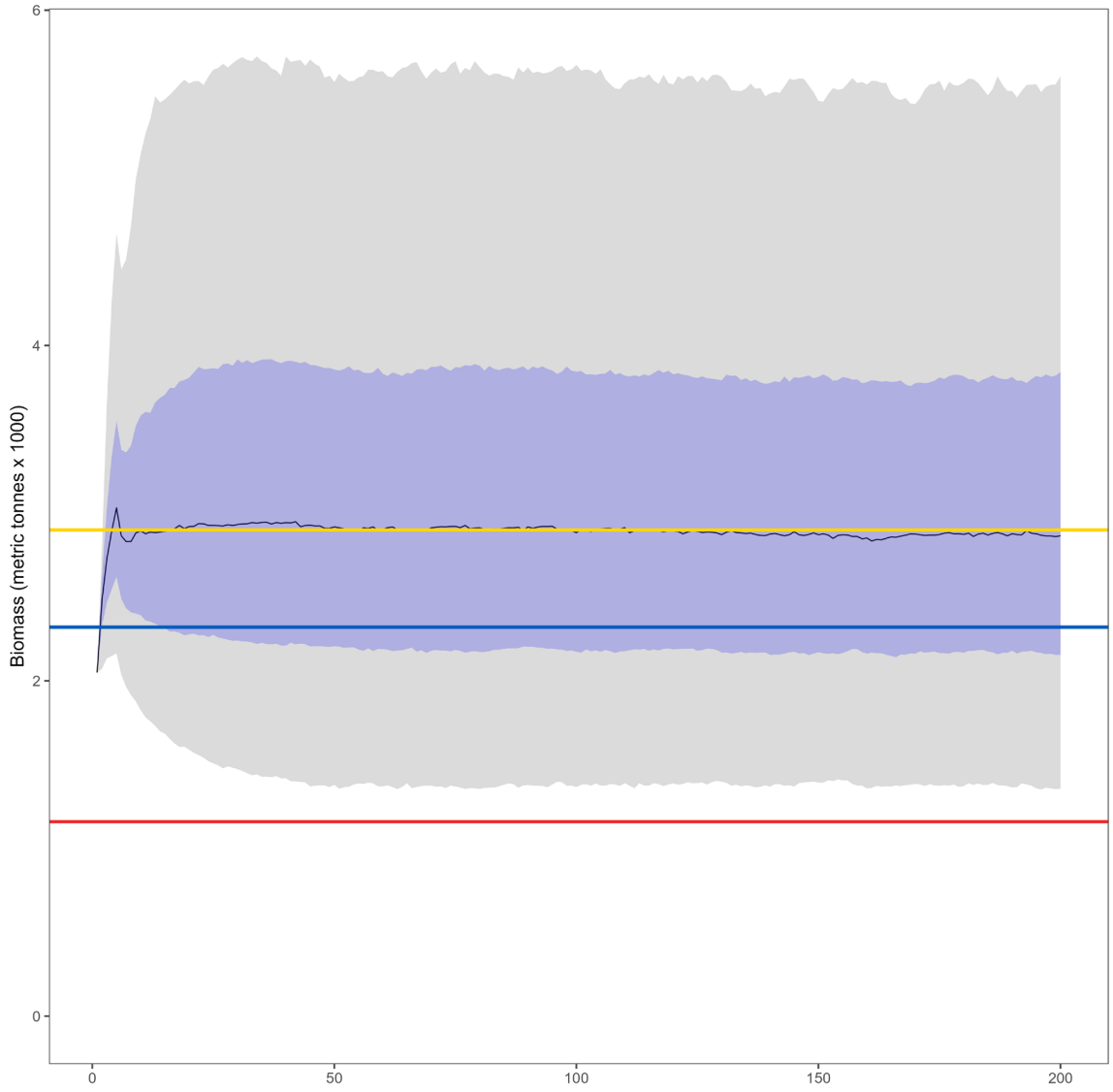

Figure 36. Harvest decision rule simulated median fully-recruited biomass estimates in SFA 25A. The blue shading represents the 50% confidence interval and the grey shading is the 90% confidence interval. The reference points used in this scenario are represented by the yellow horizontal line (target reference point), the blue horizontal line (upper stock reference; $B_{MSY(80)}$), and the red horizontal line (limit reference point; $B_{MSY(40)}$).

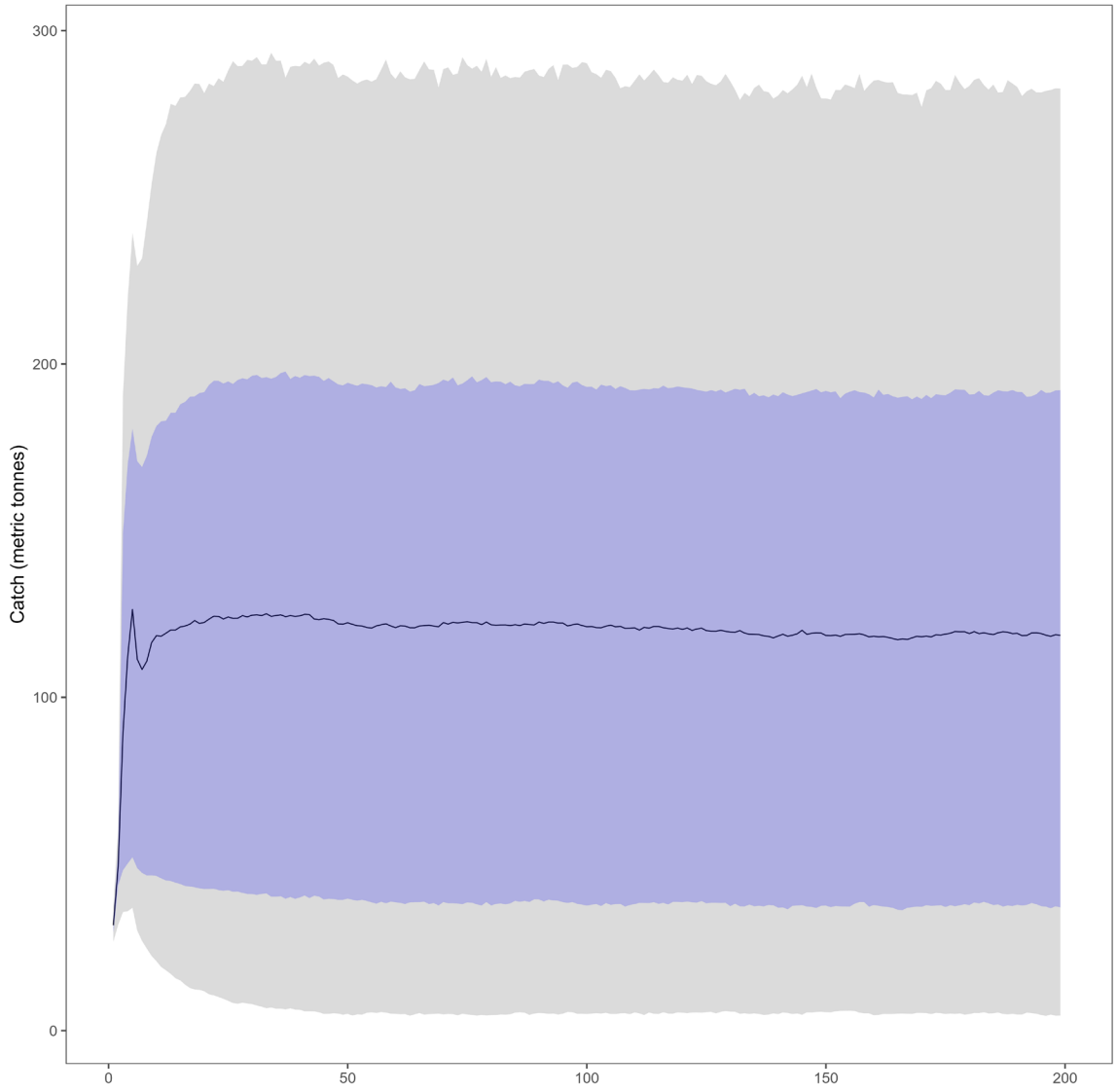

Figure 37. Harvest decision rule simulated median removal estimates in SFA 25A. The blue shading represents the 50% confidence interval and the grey shading is the 90% confidence interval.

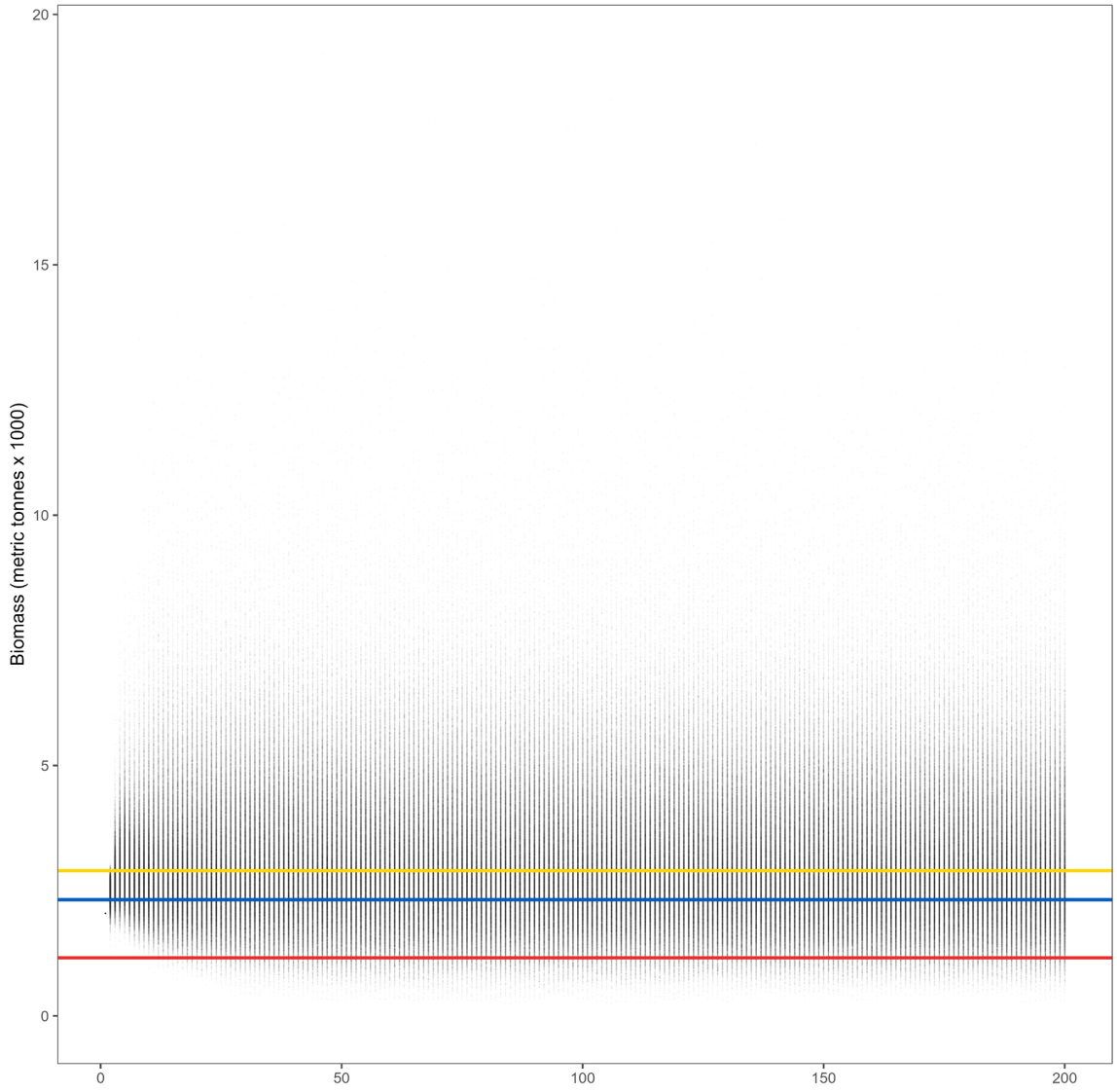

Figure 38. Harvest decision rule simulated raw fully-recruited biomass estimates in SFA 25A. The reference points used in this scenario are represented by the yellow horizontal line (target reference point), the blue horizontal line (upper stock reference; $B_{MSY(80)}$), and the red horizontal line (limit reference point; $B_{MSY(40)}$). Each grey line represents one of the 10,000 realizations.

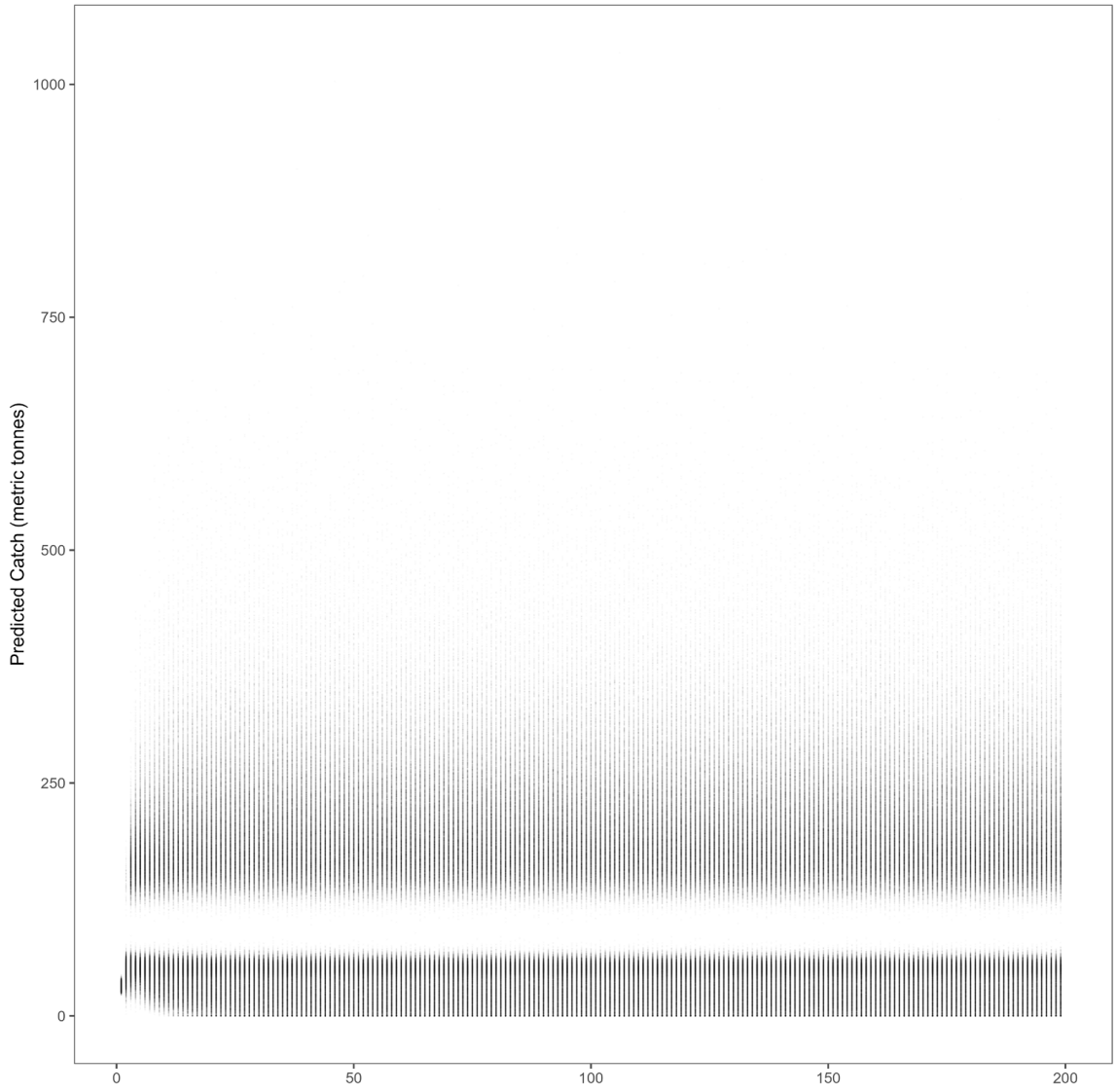

Figure 39. Harvest decision rule simulated raw removal time series in SFA 25A. Each grey line represents one of the 10,000 realizations.

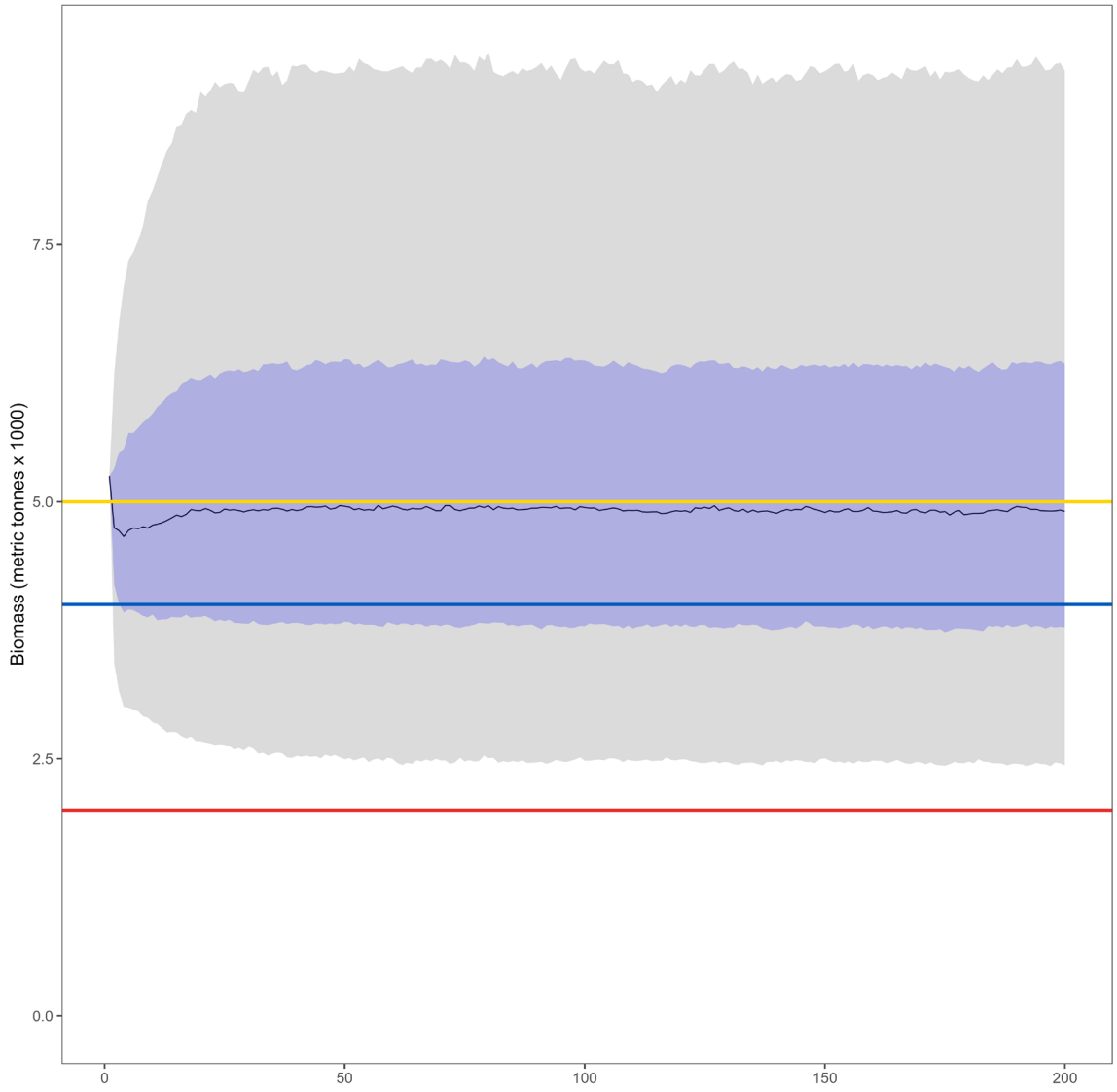

Figure 40. Harvest decision rule simulated median fully-recruited biomass estimates in SFA 26A. The blue shading represents the 50% confidence interval and the grey shading is the 90% confidence interval. The reference points used in this scenario are represented by the yellow horizontal line (target reference point), the blue horizontal line (upper stock reference; $B_{MSY(80)}$), and the red horizontal line (limit reference point; $B_{MSY(40)}$).

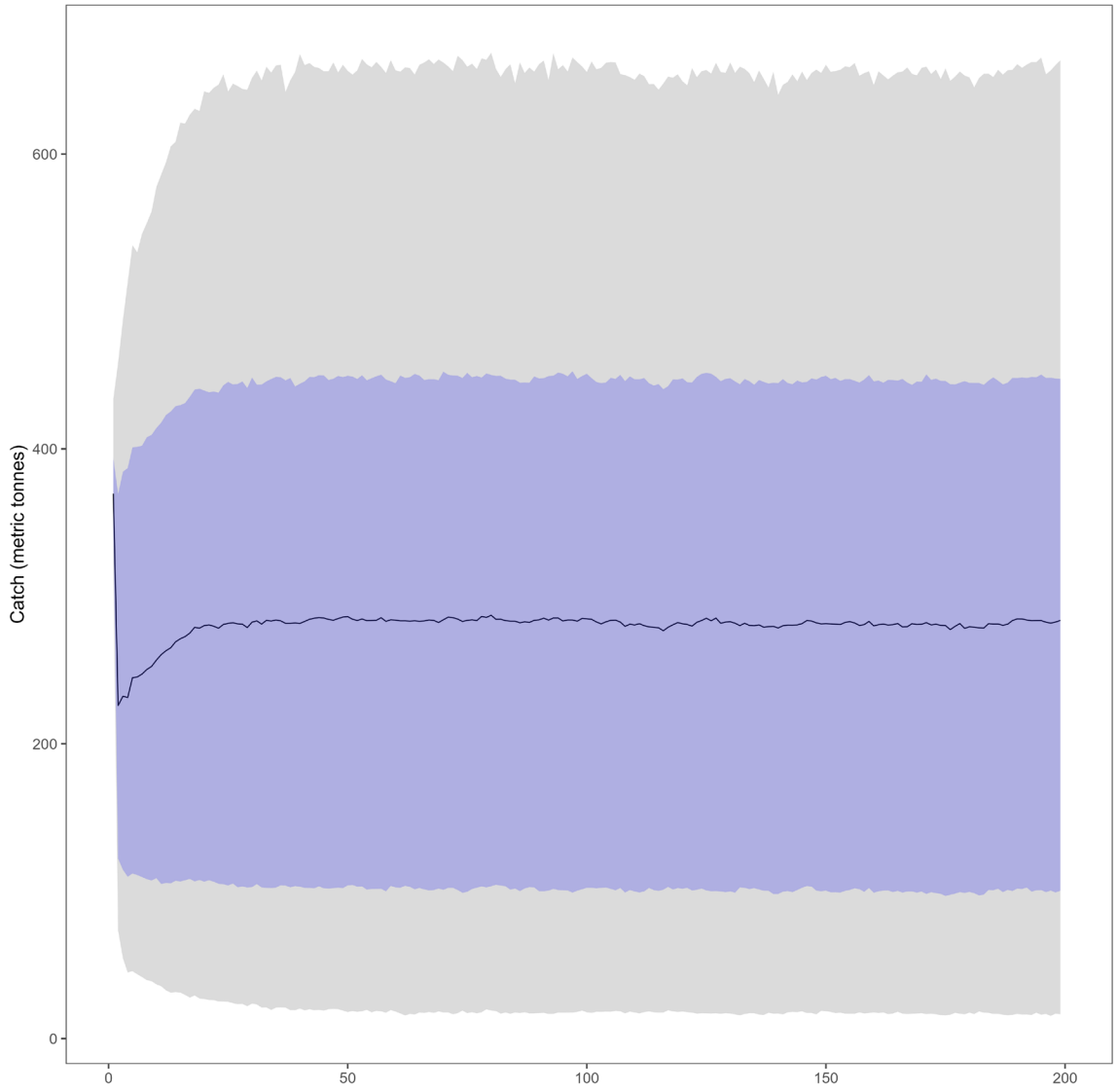

Figure 41. Harvest decision rule simulated median removal estimates in SFA 26A. The blue shading represents the 50% confidence interval and the grey shading is the 90% confidence interval.

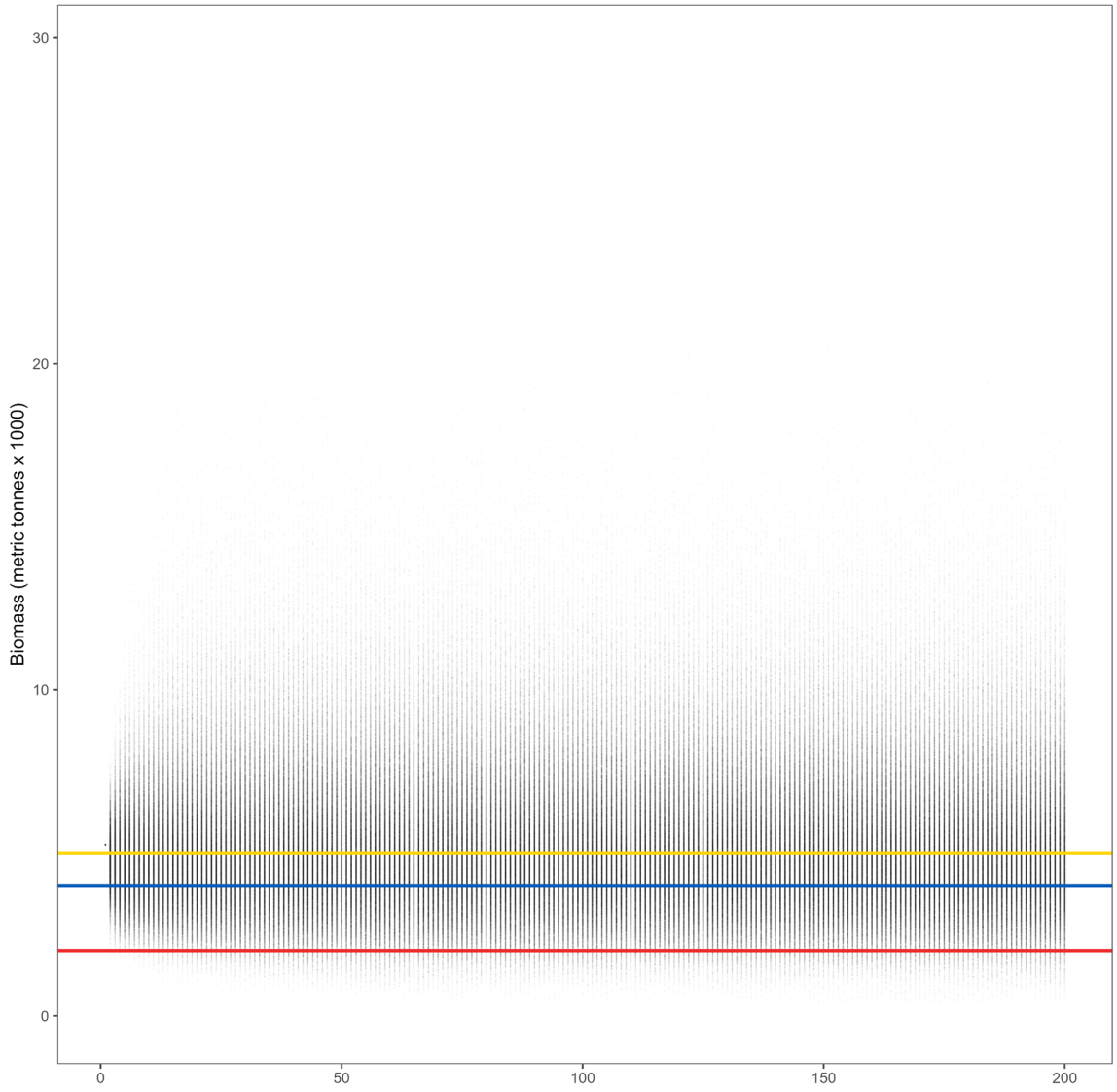

Figure 42. Harvest decision rule simulated raw fully-recruited biomass estimates in SFA 26A. The reference points used in this scenario are represented by the yellow horizontal line (target reference point), the blue horizontal line (upper stock reference; $B_{MSY(80)}$), and the red horizontal line (limit reference point; $B_{MSY(40)}$). Each grey line represents one of the 10,000 realizations.

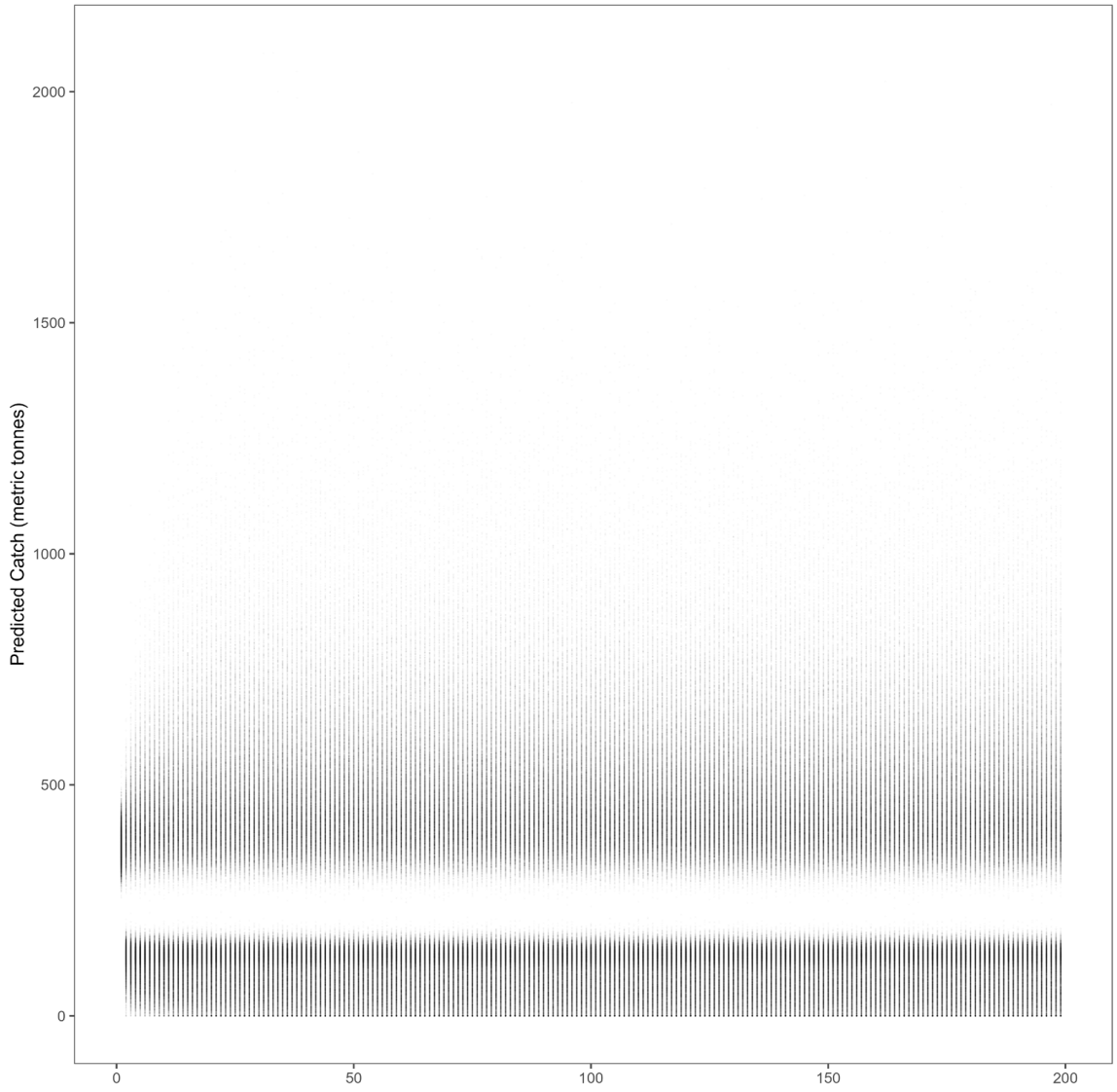

Figure 43. Harvest decision rule simulated raw removal time series in SFA 26A. Each grey line represents one of the 10,000 realizations.